Immunometabolic profiling of T cells in response to prolonged moderate intensity cycling in humans

Fendi Pradana [1,2], Jonathan P Barlow [1,3], Jack Shayler [1], Sarah K Dimeloe [4,5], Nancy Gudgeon [4,5], Tim Podlogar [1], Gareth A Wallis [1], Alex J Wadley [1*]

[1] School of Sport, Exercise, and Rehabilitation Sciences, University of Birmingham, UK
[2] Nutrition Study Program, Universitas Tadulako, Indonesia
[3] Cellular Health & Metabolism Facility, University of Birmingham, UK
[4] Institute of Immunology and Immunotherapy, College of Medical and Dental Sciences, IBR, University of Birmingham, UK
[5] Institute of Metabolism and Systems Research, University of Birmingham, UK

ABSTRACT

Background: Emerging data indicates that enrichment of peripheral blood with T lymphocytes during exercise and their associated changes in function are underpinned by modulation of cellular bioenergetics. However, there is a dearth of literature examining these responses using metabolic thresholds to prescribe exercise intensity or providing single cell resolution on immunometabolic outcome measures. Objectives: The current study was designed to examine the metabolic phenotypes and real-time bioenergetic responses to activation of enriched naïve helper ($CD4^+$) and cytotoxic ($CD8^+$) T cells and peripheral blood mononuclear cells (PBMCs) in response to prolonged cycling. Methods: Ten aerobically trained males and females (mean ± SD: age 21 ± 1 years; maximal oxygen consumption: 53.9 ± 9.8 ml · kg^{-1} · min^{-1}) undertook a 2-hour bout of continuous cycling at a power output eliciting 95% lactate threshold-1. Blood samples were collected at rest, immediately (post), and 2 hours after cycling cessation (recovery). Using injection sequences of cell respiration modulators and a CD3/CD28 activator, bioenergetic profiles of PBMCs and enriched naïve $CD4^+$ and $CD8^+$ T cells were determined using extracellular flux analysis. Mitochondrial membrane potential ($\Delta\Psi m$) was examined using flow cytometry. Results: Despite cycling evoking significant fluctuations in peripheral blood T cell numbers, there were no changes in absolute or relative measures of mitochondrial respiration, glycolytic flux and ATP synthesis rate post and recovery vs rest. Contribution of mitochondrial respiration to ATP production was greater than glycolysis in naïve T cells across all timepoints, but not PBMCs in recovery. This was despite absolute and relative changes in $\Delta\Psi m$ of memory T cells being greater in recovery vs. rest. Bioenergetic responses to ex vivo T cell activation were not different between cell types or timepoints. Conclusion: These data indicate that the metabolic phenotypes of naïve T cells and PBMCs were largely unaltered within 2 hours of prolonged moderate intensity cycling.

**Corresponding author:*
Dr Alex J Wadley
School of Sport, Exercise & Rehabilitation Sciences
University of Birmingham
Edgbaston
Birmingham, UK
B15 2TT
Email: a.j.wadley@bham.ac.uk
Phone: +44 (0)121 414 8011

INTRODUCTION

Single bouts of exercise promote the preferential mobilisation of lymphocytes primed for migration to central and peripheral tissues. These include skeletal muscle (16) and work in animals indicates that lymphoid sites of foreign antigen encounter, such as the lung and Peyer's patches accumulate T cells after exercise cessation (37). Trafficking of lymphocytes in this manner is believed to facilitate remodelling of these tissues; however, the underpinning mechanisms are unclear. In 1958, it was first reported using respirometry that moderate intensity exercise increased peripheral blood mononuclear cell (PBMC) oxygen consumption in humans (5). Recent advances in real-time extracellular flux analysis (EFA) have permitted more comprehensive profiling of substrate metabolism from intact immune cells by measuring oxygen flow in response to various mitochondrial agents. In PBMCs isolated immediately after vs. before exercise, it has been reported that swimming exercise to exhaustion increased basal respiration (72) and low-intensity cycling (~35% $\dot{V}O_{2peak}$)increased basal and fatty acid-dependent respiration (41). Other studies have reported no changes in PBMC respiratory states immediately after steady state (75) and exhaustive exercise (72), notably when normalised to the number of PBMCs within peripheral blood. PBMCs are composed of diverse sub-populations of lymphocytes and monocytes with unique functions and distinct metabolic profiles (8, 12, 20, 46, 66). Moreover, bouts of exercise evoke an immediate increase in peripheral blood lymphocyte concentrations, followed by a decrease in recovery (≈1-3 hours) as differentiated lymphocytes with a cytotoxic phenotype leave the bloodstream. This presents a challenge when sampling cells for evaluation of their metabolism and conclusions have largely been drawn from mixed cell populations, i.e., PBMCs. One study by Lu et al, 2022 demonstrated that maximal and reserve oxygen consumption rate (OCR) were increased in immunomagnetically enriched natural killer (NK) cells isolated from the PBMC fraction after vs. before exhaustive cycling. This study also reported that after 6 weeks of regular exercise training, maximal and reserve OCR were increased in NK cells at rest (42). Other studies have similarly documented a relationship between aerobic fitness and basal and maximal PBMC respiration (2, 32) and mitochondrial mass was higher in naïve cytotoxic ($CD8^+$) T cells isolated from active vs. inactive individuals (1). Immune cell metabolism is evidently remodelled with exercise training; however, due to marked compositional shifts in PBMCs, limited work has examined cell-by-cell bioenergetic changes in response to single bouts of exercise, notably in T cells.

Helper ($CD4^+$) T cells serve broadly to orchestrate immune response via cytokine signalling (e.g., interleukin (IL)-2, interferon-gamma and tumour necrosis factor-alpha), whereas $CD8^+$ T cells eliminate cancerous or virus infected cells through the release of cytotoxic molecules. It is now established that cellular metabolism is modulated to meet the bioenergetic and biosynthetic demands needed to govern these T cell processes (81). The metabolic pathways used to generate ATP in T cell subsets are dependent on the degree of antigen experience (56). Naïve T cells are antigen inexperienced cells generated in the thymus that mostly rely on mitochondrial respiration to fulfil their primary function of recirculating through lymphoid tissues to survey for antigens (47). Upon T cell receptor (TCR) engagement and co-stimulatory CD28 ligation, a pronounced glycolytic shift facilitates T cell effector functions and subsequent differentiation into memory T cells (24, 57, 80). Antigen encounters therefore result in central memory (CM), effector memory (EM) and terminally differentiated effector memory (TEMRA) T cells exhibiting increasingly greater reliance on glycolysis than naive T cells for basal respiration (TEMRA > EM > CM > naïve). Enrichment of peripheral blood with antigen experienced T cells with higher basal respiration may therefore influence the metabolic activity of the PBMC fraction during exercise and make changes within individual T cell subsets difficult to discern (72). Perturbations in T cell energetics are permissible given the multiple immunological stressors associated with exercise at the cellular, systemic, and tissue level. A recent study employing single cell RNA sequencing reported that genes associated with metabolic regulation were enriched in $CD4^+$ and $CD8^+$ T cells after maximal exercise, most notably in EM (3). These changes were aligned with upregulation of genes associated with cell migration, antigen binding, and cytokine production. Other data indicate that exercise-mobilised T cells are primed to uptake energy substrates such as glucose (75), and this may facilitate modulation of their metabolic activity to fulfil these effector functions.

Most studies examining immunometabolic responses to exercise have evaluated changes in PBMCs immediately after bouts ≤1 hour. A recent scoping review specifically highlighted that there is a dearth of literature examining immunometabolic responses in individual T cell subsets after prolonged exercise into recovery (63). By using prior cell sorting, EFA can provide this single cell resolution (38, 58, 64). Furthermore, contemporary flow cytometry permits interrogation of cellular metabolism by coupling metabolic indicators of mitochondrial membrane potential ($\Delta\Psi m$) to T cell immunophenotyping, providing cell-by-cell measurements (25).

This study was designed to examine the metabolic sensitivity of T cell subsets to prolonged moderate intensity cycling compared to the PBMC fraction. Naïve $CD4^+$ and $CD8^+$ T cells were a specific focus of EFA given that these cells are mobilised into peripheral circulation during exercise, abundant within the PBMC fraction and metabolically adaptable to exercise training (1), thus providing a robust single cell model to examine immunometabolic responses to exercise. Previous studies in this area have largely prescribed exercise intensity based on a fixed proportion of maximal oxygen consumption ($\dot{V}O_{2max}$) (32, 42); however, this doesn't account for inter-individual variability in substrate uptake and oxidation during exercise, which might govern subsequent immunometabolic responses. Prescribing intensity at the upper limit of moderate exercise intensity domain, demarcated by lactate threshold-1 (LT1 - exercise intensity at which there is a measurable increase in blood lactate concentration) would facilitate comparable relative metabolic stress between participants (30, 31, 40). Accordingly, the aims of this study were to 1) evaluate the metabolic phenotypes of immunomagnetically enriched naïve $CD4^+$ and $CD8^+$ T cells and PBMCs using extracellular flux analysis; 2) quantify $\Delta\Psi m$ of these T cell subsets using flow cytometry; 3) examine real-time metabolic, morphological and cytokine responses to *ex vivo* T cell activation and 4) draw as-

sociations of these outcomes with circulating T cell substrates (glucose, glutamine, and triglycerides) in response to 2 hours of cycling at 95% LT1.

MATERIALS AND METHODS

Participants

Ten participants (5 males and 5 females) gave written informed consent to take part in this study (Table 2). Participants underwent screening prior to enrolment to include individuals who were physically active as defined by the General Practice Physical Activity Questionnaire (GPPAQ) (21), and exceeded an aerobic fitness threshold for males (> 50 ml · kg^{-1} · min^{-1}) and females (> 35 ml · kg^{-1} · min^{-1}) (77). All experimental visits for female participants were conducted at the same phase of menstrual cycle to prevent the influence of estrogen on immunometabolic markers (52). Participants were excluded if they were smokers, currently taking medication/s, eating a ketogenic diet, had donated blood in the last 3 months, or had a history of cardiovascular, metabolic, neurological, or inflammatory disease.

Study Design

The study was a randomised crossover design, comprising four morning visits at the School of Sport, Exercise and Rehabilitation Sciences at the University of Birmingham, conforming to the Declaration of Helsinki, except for prior registration on a publicly accessible database (85). After an initial screening visit to determine LT and $\dot{V}O_{2max}$, participants undertook three randomised visits, consisting of two identical cycling trials (CT-1 and CT-2) and one rest trial (REST), each separated by 7 days (Figure 1). Our preliminary data indicated differences in real-time glycolytic responses to T cell activation based on blood sample processing (0-4 hours after collection) and temperature (room temperature or 37°C) of metabolic assays (data not shown). Given that T cell metabolism was to be examined over a 4-hour period, the study protocol was designed to equalise time spent preparing T cell metabolic assays and eliminate the effect of blood 'sitting time'. Therefore, primary blood samples were collected on different trials at rest or 'Pre-Ex' (REST), immediately after or 'Post-Ex' (CT-1), and 2 hours after or 'Recovery' (CT-2) cycling and processed immediately at room temperature. CT-1 and CT-2 were differentiated only by the timing of these blood sample withdrawals after cycling cessation, and conducted under identical conditions, with the aim of eliciting comparable physiological and immunological responses. These were confirmed by monitoring gas exchange data and drawing secondary blood samples at every timepoint throughout CT-1 and CT-2 respectively (details below). Between all trials, lifestyle factors that might influence immunity were subjectively monitored, including illness symptoms, anxiety, and sleep quality.

All visits started at the same time of day for each participant (range: 6:30–8.00 AM) and were conducted under stable climatic conditions (temperature (°C): 21.0 ± 0.6, humidity (%): 39.1 ± 10.0 and barometric pressure (hPa): 1002.1 ± 12.7). Participants were asked to refrain from vigorous exercise, and the consump-

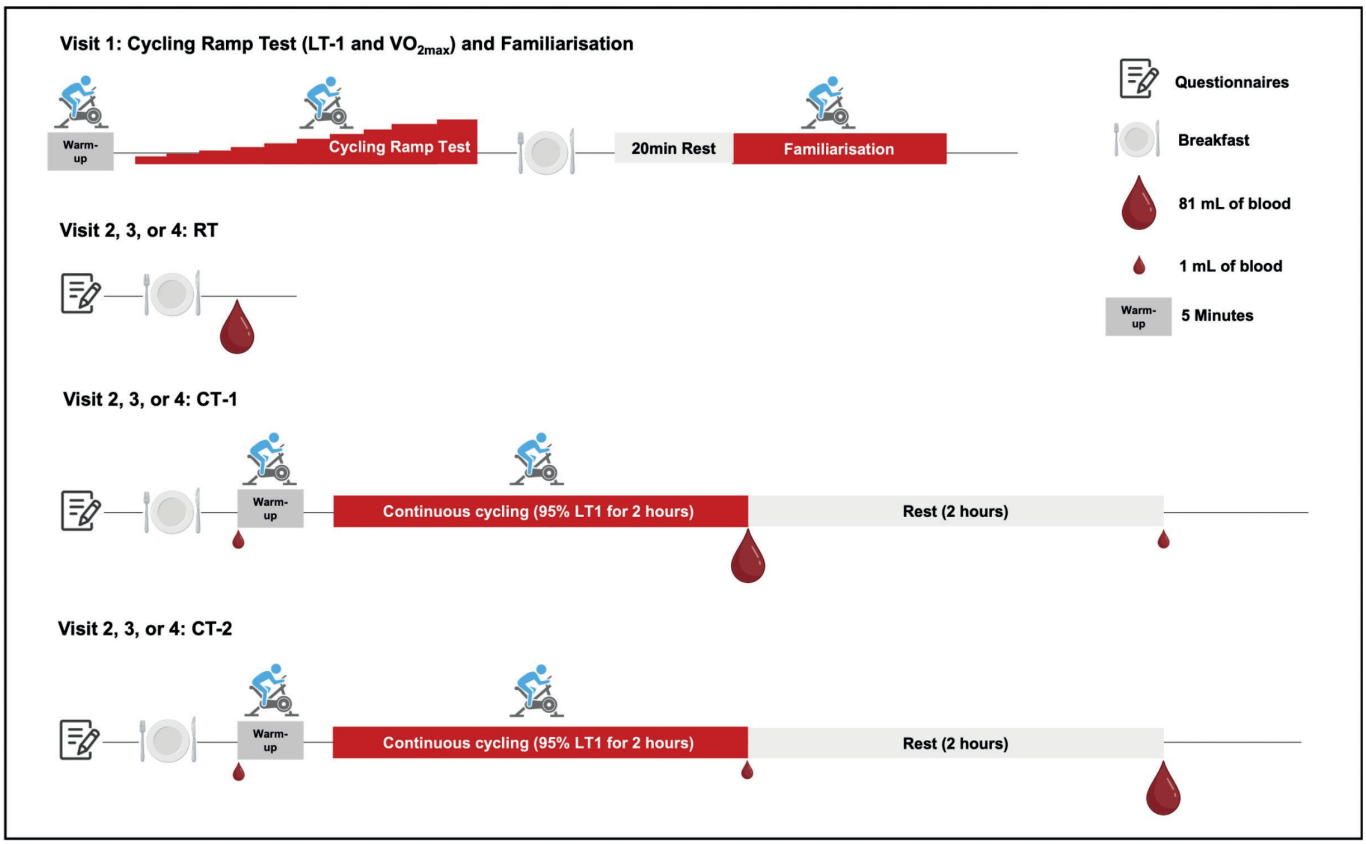

Figure 1. Study schematic illustrating a time axis for each of the 4 laboratory visits. On visit 1, a cycling ramp test to exhaustion was used to determine lactate threshold-1 (LT1) and maximal oxygen consumption (VO_{2MAX}). Participants then undertook 3 randomised trials, including Rest (RT) and cycling trials 1 and 2 (CT-1 and CT-2). Blood sampling is indicated with small droplets (1 mL) for samples collected for determination of complete blood cell count and large droplets (77 mL) for all other outcomes. Key indicates when breakfast, questionnaires, warm-up and rest periods took place. Created with BioRender.com.

tion of caffeine and alcohol for 48 hours prior to attending each visit. Furthermore, to standardise nutrition, participants were asked to record their food intake for 24 hours before the first visit and to replicate this diet for all subsequent visits, as well undertaking an overnight fast from 10pm, consuming only water (ad libitum) during this period. Participants were provided with a breakfast of oats mixed with semi-skimmed milk (normalised for carbohydrate content: 1 g · kg^{-1} body mass) (6, 76) to ensure the energy and macronutrient intake across trials and between participants was standardised.

Screening Visit (Visit 1)

Participants attended the laboratory for screening and determination of LT and $\dot{V}O_{2max}$. Body mass (Ohaus CD31, New Jersey, USA), height (Seca Alpha, Hamburg, Germany) and resting blood pressure (Thuasne BP 3W1-A, Taipei, Taiwan) were recorded. An exercise tolerance test was then conducted on an electromagnetically braked cycle ergometer (Excalibur, Lode, Netherlands). After a warm-up for 5 minutes at a rating of perceived exertion (RPE) of 8–10 using the Borg scale (61), participants commenced cycling at 70 watts and then 30-watt increments were added every 4 minutes until volitional exhaustion (RPE = 20). A breath-by-breath system (Vyntus, Vyaire Medical, IL, US) was used for continuous measurement of oxygen uptake, and fingertip blood lactate measurements were made at the end of every 4-minute stage (Lactate Pro 2, Arkray, Kyoto, Japan). Participants were asked to maintain a pedal cadence > 60 and encouragement was given by the research team. $\dot{V}O_{2max}$ was calculated using gas exchange data from the final stage and expressed relative to body weight (ml · kg^{-1} · min^{-1}) (28). Participants were provided with breakfast and during this time, LT software (36) was used to determine the power output that elicited a 0.5 mmol · L^{-1} increase in lactate above baseline value, thus defining LT1 (30, 31). A 15-minute familiarisation was then conducted at a power output eliciting 95% of LT1 and a final blood lactate measurement made to confirm the correct intensity for subsequent trials.

Experimental Trials (Visits 2-4)

In the morning of each trial (REST, CT-1, and CT-2), participants were asked to complete questionnaires evaluating illness symptoms (48) state and trait anxiety (71) and sleep efficiency (percentage of time asleep relative to the amount of time spent in bed) (11) during a 30-minute period of rest (Pre-Ex). During this time, blood pressure and body mass were also measured. A standardised breakfast was provided as described above and then a catheter (Becton, Dickson & Company, Oxford, UK) inserted into the antecubital vein of the forearm to obtain a resting blood sample 15 minutes after feeding. Each exercise trial commenced with a 5-minute warm-up at a RPE of 8–10, followed by 2-hours of continuous-cycling at a power output eliciting 95% LT1 (CT-1 or CT-2). Every 15 minutes during CT-1 and CT-2, exercise intensity was confirmed by measuring $\dot{V}O_2$ uptake for 3 minutes and heart rate (H10, Polar Electro, Finland), RPE and the affective response (26) recorded. Energy expenditure, carbohydrate and fat oxidation were calculated based on gas exchange data (33). Following completion of CT-1 and CT-2, participants remained seated in the laboratory for a 2-hour recovery period.

Blood Sampling

A total of seven blood samples were taken across the 3 trials, including a single blood draw during REST (Pre-Ex) and 3 blood draws during CT-1 and CT-2 (Pre-Ex, Post-Ex, and Recovery). The catheter was kept patent through regular flushes with saline (0.9% NaCl, Becton, Dickson & Company, Oxford, UK). The volumes of blood drawn at each timepoint varied depending on the trial (Figure 1). During REST (Pre-Ex), immediately after CT-1 (Post-Ex) and 2 hours post-exercise in CT-2 (Recovery), 70 mL of blood was collected into sodium heparin vacutainers (Becton, Dickson & Company, Oxford, UK) for isolation of peripheral blood mononuclear cells (PBMCs). Additionally, 6 mL of blood was collected into K_2EDTA vacutainers (Becton, Dickson & Company, Oxford, UK) and 4 mL into clotting vacutainers (Becton, Dickson & Company, Oxford, UK) for isolation of plasma and serum at these 3 timepoints, respectively. Across all seven timepoints, 1 mL of blood was collected into K_2EDTA vacutainers (Greiner Bio-One, Frickenhausen, Germany) to obtain a complete blood cell count using an automated haematology analyser (Yumizen H500, Horiba, Kyoto, Japan). These data were obtained to ensure comparable leukocyte counts at rest (REST vs. CT-1 vs. CT-2) and in response to prolonged cycling (CT-1 vs. CT-2).

Blood Processing and Immunomagnetic Separation of Naïve T Cells

PBMCs were isolated by density gradient centrifugation and then naïve $CD4^+$ and $CD8^+$ T cells enriched using magnetic activated cell sorting (MACS) microbead isolation kits (Cat #130-045-101 and Cat #130-093-244, Miltenyi Biotec, Bergisch Gladbach, Germany) (82). Purity of each cell fraction was confirmed using flow cytometry. All methods and the gating strategy for naïve, CM, EM and TEMRA T cells are presented in Supplemental Figure 1. Whole blood in clotting tubes was left for 15 minutes at room temperature and then centrifuged alongside K_2EDTA blood collection tubes for 10 minutes at 1,525 x g at 4 °C for isolation of serum and plasma respectively. Both serum and plasma were then aliquoted and stored at -80 °C until subsequent analysis.

Immunophenotyping and Assessment of Mitochondrial Membrane Potential

Assay Conditions

Fluorescently conjugated antibodies and the mitochondrial indicator (MI) MitoSpy Orange chloromethyl-tetramethylrosamine (MSO, Cat# 424804, Biolegend) were combined to quantify the $\Delta\Psi m$ of naïve, CM, EM and TEMRA $CD4^+$ and $CD8^+$ T cell subsets using nine-colour flow cytometry (Beckman Coulter, California, USA) (25, 54). Peripheral blood T cell concentrations (cells/µL) were also determined and adjusted for changes in blood volume (44). MSO is a cationic compound that passively diffuses across the plasma membrane and accumulates in mitochondria based on its electrochemical gradient, thus serving as a surrogate for mitochondrial activity. A separate sample was stained under identical conditions, but with BAM-15 to uncouple mitochondria and permit measurement of baseline MSO mean fluorescence intensity (MFI). MSO was monitored by the λ610 nm laser and λ585/42nm detector. MitoView Green (Cat # 70054, MVG, Cambridge Biosciences) was monitored on the λ488 nm laser and λ525/40nm detector to quantify mitochondrial mass. Full details of antibody and MI staining and flow cytometry gating are described in supplementary materials.

Calculations (Cell concentrations and ΔΨm)

Peripheral blood cell concentrations were calculated by combining automated haematology analysis (lymphocyte concentration)

with individual T cell subset frequencies determined by flow cytometry. All concentrations were adjusted for changes in blood volume using the formula proposed by Matomäki et al, 2000 (44) and expressed as cells per µL. Within each cell subset, ΔΨm was expressed as a ratio of the raw MFI of MSO to the BAM-15 treated control. Both absolute and relative changes (vs. Pre-Ex) in ΔΨm were then calculated. Mitochondrial mass was monitored across timepoints by quantifying the MFI of MVG within each T cell subset.

Real-time metabolic profiling

Experimental assays were carried out using the Seahorse XFe96 extracellular flux analyser and pre-designed using Seahorse analytics software 1.0.0-570 (Agilent Technologies, USA). A metabolic profiling assay (Figure 3A–B) was used to examine the bioenergetic profile of PBMCs, enriched naïve $CD4^+$ and $CD8^+$ T cells (via OCR and ECAR measurement) using an injection sequence of different cell respiration modulators (Oligomycin, BAM 15, Rotenone and Antimycin A) (45). A T cell activation assay (Figure 5C–E) was coupled to this by injecting anti-human CD3/CD28 soluble antibody complexes to evaluate real time bioenergetic responses, measured via changes in PER and OCR (35, 47). The assay preparation and injection strategies are outlined separately below for simplicity.

Mito Stress Assay

Preparation

A Seahorse XFe96 sensor cartridge was hydrated in 200 µL/well of XF Calibrant in a non-CO_2 incubator overnight at 37°C. The day after, Seahorse XFe96 extracellular flux analyser was calibrated for minimum 5 hours prior to starting the assay. PBMCs, enriched naïve $CD4^+$ and $CD8^+$ T cells (2 x 10^5 cells/well) were suspended in 50 µL of pre-warmed Seahorse XF RPMI assay medium (supplemented with 10 mM glucose, 1 mM pyruvate, and 2 mM glutamine, pH = 7.4, Agilent Technologies, USA) and seeded onto a Seahorse XFe96 cell culture microplate (Agilent Technologies, USA). A total of 4 technical replicates were used for each assay. Each well was pre-coated with sterile Cultrex Poly-D-lysine (Bio-techne, Minneapolis, USA). The plate was centrifuged at 300 x g for 5 minutes at room temperature with the brake off and the plate rested for 1 hour in a non-CO_2 incubator at 37°C. Assay medium (130 µL) was added 15 minutes prior to starting experiments.

Assay Injection Strategy

Injected reagents (20 µL/well) were prepared including 2 µg · mL^{-1} Oligomycin (Sigma-Aldrich, Merck, UK) in port A, 3 µM BAM 15 (TOCRIS, Minneapolis, USA) in port B and a mixture of 2 µM Rotenone + 2 µM Antimycin A (Sigma-Aldrich, Merck, UK) in port C. The experimental plate was then inserted into the analyser, and an induced real-time ATP rate (pmol · min^{-1}) assay was performed. Following the pre-design experimental assay, OCR (pmol · min^{-1}) and ECAR (mpH · min^{-1}) were measured 14 minutes after the assay begun reflecting the baseline measurement (3 cycles) and following each of 3 consecutive injections over a 40-measurement period (Figure 3B). Injections of Oligomycin (port A, 3 cycles) after 15–28 minutes, BAM 15 (port C, 3 cycles) after 29–41 minutes and a mixture of Rotenone + Antimycin A (port C, 3 cycles) after 42–54 minutes were implemented to provide a detailed metabolic profile including mitochondrial respiration, glycolytic and ATP synthesis rate for each sample.

Calculations

Data are resented in absolute values per 2 x 10^5 cells as OCR (pmol O_2 · min^{-1}), Glycolytic PER (pmol H^+ · min^{-1}) and ATP synthesis rate (pmol ATP · min^{-1}). Calculations were then performed to define respiratory parameters, which are provided in Table 1 and visually depicted in Figure 3A. Absolute values for naïve $CD4^+$ and $CD8^+$ T cells were coupled to T cell frequencies determined by flow cytometry to calculate the contribution of naïve $CD4^+$ and $CD8^+$ T cells to each metabolic outcome within the PBMC fraction. In addition, relative contributions of OCR (% of total and % of maximum) and ATP synthesis rate (% of total) were determined separately for each cell fraction.

Table 1. Calculation of respiratory parameters measured by Seahorse extracellular flux analyser

Parameter	Calculation
Basal mitochondrial respiration	OCR without any injections minus OCR after addition of rotenone and antimycin A.
Proton leak	OCR after oligomycin injection minus OCR after addition of rotenone plus antimycin A.
Maximal mitochondrial respiration	OCR after injection of BAM15 minus OCR after addition of rotenone plus antimycin A
Spare respiratory capacity	Maximal mitochondrial respiration minus basal mitochondrial respiration
ATP-linked respiration	Basal mitochondrial respiration minus proton leak
Non-mitochondrial respiration	OCR after the injection of rotenone plus antimycin a
Mitochondrial PER	Basal mitochondrial respiration (OCR) multiplied by 0.61 (CO_2 contribution factor)
Glycolytic PER	Total PER minus mitochondrial PER
Mitochondrial ATP synthesis rate	ATP-linked respiration (corrected for a 10% overestimation of proton leak due to oligomycin-induced hyperpolarisation of mitochondrial inner membrane) multiplied by 5.45 (P/O_2 ratio for glucose) plus basal mitochondrial respiration multiplied by 0.242 (P/O_2 ratio for TCA flux). We have accounted for mitochondrial ATP driven by reducing equivalents generated during both glycolysis and the oxidation reactions of pyruvate dehydrogenase plus the tricarboxylic acid cycle, and substrate-level phosphorylation at succinyl-CoA synthetase during activity of the tricarboxylic acid cycle.
Glycolytic ATP synthesis rate	Glycolytic PER (pmol H^+/min) using 1:1 stoichiometry for H^+ and lactate. We did not include pyruvate oxidation to bicarbonate in glycolytic ATP calculations.
ATP synthesis rate	Glycolytic ATP synthesis rate + mitochondrial ATP synthesis rate
Abbreviations: OCR, oxygen consumption rate; ATP, adenosine triphosphate; PER, proton efflux rate; P/O ratio, phosphorylated per atom of oxygen.	

T cell Activation Assay

Assay Injection Strategy

A T cell activation assay was used to examine real-time metabolic responses to activation and followed identical preparation procedures to the Mito stress assay. PER (pmol · min^{-1}) and OCR (pmol O_2. min^{-1}) were measured 14 minutes after the assay baseline measurement (3 cycles) and following each of 2 consecutive injections over a 100-minute period (Figure 5C–E). A human Im-

munoCult CD3/CD28 activator (Catalog # 10991, STEMCELL Technologies, Cambridge, UK) or assay media were injected at 20 µL/well (port A, 10 cycles) after 15–79 minutes and then the glucose analog 2-Deoxy-D-glucose (2-DG, Thermo Scientific, UK) injected after 80–120 minutes (port B, 4 cycles). The injection of 2-DG caused a rapid inhibition of glycolysis and subsequent decrease in PER, thus providing confirmation that prior changes in PER were primarily due to glycolysis (70).

Calculations

Data were presented in absolute values per 2 x 10^5 cells as Glycolytic PER (pmol $H^+ \cdot min^{-1}$), ATP-linked respiration based on OCR (pmol $O_2 . min^{-1}$), and ATP synthesis rate (pmol ATP $\cdot min^{-1}$). Data were calculated following the formula provided in Table 1 and visually depicted in Figure 5C–E).

Ex Vivo T-cell Stimulation

Under sterile conditions, PBMCs and enriched naïve $CD4^+$ and $CD8^+$ cells (2 x 10^5 cells/well) were suspended in 180 µL of pre-warmed ImmunoCult-XF T-cell expansion medium (STEMCELL Technology, UK) and seeded onto a non-treated 96-well round bottomed microplate (Fisher Scientific, UK). Into each well, 20 µL of ImmunoCult human CD3/CD28 T-cell activator (Catalog # 10991, STEMCELL Technologies, Cambridge, UK) or 20 µL of expansion medium (control well) was gently mixed with the cells and incubated for 12 hours at 37 °C (5% CO_2). All cell suspensions were centrifuged at 300 x g for 5 minutes at room temperature to harvest cells for measurement of post-activation diameter (µM) using a dual fluorescence cell counter (Nexcelom Bioscience, Massachusetts, USA), and quantify interleukin 2 (IL-2) in the supernatant from activated naïve T cells using high sensitivity ELISA kits (Bio-techne, Minneapolis, USA, Cat# HS200).

Metabolic Substrates

The concentrations of glucose and glutamine in plasma, and triglyceride in serum were quantified at all timepoints using bioluminescent rapid assay kits (Promega, Madison, USA). Lactate was measured at Rest and throughout CT-1 and CT-2, but not Recovery (Lactate Pro 2, Arkray, Kyoto, Japan).

Statistical Analysis

GraphPad Prism 10.2.2 analysis software (San Diego, CA) was used to perform statistical analysis and graph creation. Data were assessed for normal distribution using the Shapiro-Wilk test. Normally distributed variables were analysed across exercise trials (REST, CT-1, and CT-2), timepoints (Pre-Ex, Post-Ex, and Recovery) and cell types (PBMCs, naïve $CD4^+$ and $CD8^+$ T cells) by mixed-effects two-way analysis of variance (Two-way ANOVA). Post hoc analyses of any interaction effects (e.g., Trial x Time or Time x Cell Type) were performed by a test of multiple comparisons, with either Tukey test, depending on variable normality. One-way analysis of variance (One-way ANOVA) was used to analyse peripheral blood immune cell concentrations, immunometabolic outcomes and metabolic substrates between timepoints (Pre-Ex, Post-Ex, and Recovery). In addition, t-tests were used to analyse the differences in physiological data between CT-1 and CT-2. Data that were not normally distributed were analysed using Wilcoxon or Kruskal-Wallis's test. Statistical significance was accepted at the $p < 0.05$ level. All values are presented as means ± standard deviation (SD). To assist with interpretation of changes in immunometabolic outcomes, 95% confidence intervals (CI) and effect sizes (Cohen's d) were computed and presented in Supplementary Materials. Effect sizes of 0.2, 0.5 and 0.8 were considered small, moderate and large respectively (13, 43).

RESULTS

Participant Characteristics, Sleep Efficiency and Anxiety

Mean participant characteristics including anthropometrics, cardiorespiratory fitness, maximal and LT1 power output are reported in Table 2. A repeated measures ANOVA showed no significant differences in sleep efficiency ($F_{1,11} = 1.87$, $p = 0.20$), state anxiety ($F_{2,15} = 0.69$, $p = 0.49$) or trait anxiety ($F_{2,17} = 0.23$, $p = 0.79$) (Table 3). Sleep efficiency and anxiety were therefore not included as covariates in subsequent statistical analyses of primary and secondary variables.

Physiological Responses to Exercise and Workload Measurements

Physiological data, estimates of energy expenditure and subjective perceptions during CT-1 and CT-2 are presented in Table 4. A paired T-test revealed no significant differences in average HR ($t(9) = 0.83$, $p = 0.43$), absolute $\dot{V}O_2$ uptake ($t(9) = 0.84$, $p = 0.42$), relative $\dot{V}O_2$ uptake ($t(9) = 0.84$, $p = 0.42$), total energy expenditure ($t(9) = 0.38$, $p = 0.71$), carbohydrate oxidation ($t(8) = 0.22$, $p = 0.83$), fat oxidation ($t(8) = 0.30$, $p = 0.77$), affective response ($t(9) = 1.77$, $p = 0.11$) or RPE ($t(9) = 0.56$, $p = 0.59$) between CT-1 and CT-2, demonstrating consistent physiological

Table 2. Participant characteristics

Variable	Male (n = 5)	Female (n = 5)
Age (years)	20.60 ± 1.14	20.80 ± 1.10
Height (cm)	185.70 ± 5.94	164.80 ± 4.16
Body mass (kg)	69.81 ± 9.03	61.89 ± 5.07
BMI ($kg \cdot m^2$)	20.17 ± 1.47	22.79 ± 1.70
$\dot{V}O_{2max}$ ($mL \cdot kg^{-1} \cdot min^{-1}$)	60.26 ± 2.74	47.63 ± 10.40
Maximum Power output (W)	299.10 ± 43.74	225.78 ± 33.61
Power output at LT-1 (W)	156.42 ± 31.54	142.40 ± 23.29

For consistency of all tables, SDs and significance lists have 1-line spacing form abbreviation. Example: Data displayed as mean ± SD.

Abbreviations: BMI, body mass index; $\dot{V}O_{2max}$, maximum rate of oxygen uptake; LT, lactate threshold.

Table 3. Sleep efficiency and state and trait anxiety score prior to each experimental trial

	Experimental Trial			
Variable	**RT**	**CT-1**	**CT-2**	**p-Value**
Sleep Efficiency (%)	83.80 ± 11.74	83.83 ± 8.06	88.60 ± 4.48	> 0.05
Anxiety State ($S_{anxiety}$)	44.40 ± 2.07	45.80 ± 4.87	45.40 ± 3.41	> 0.05
Anxiety Trait ($T_{anxiety}$)	45.00 ± 5.50	45.10 ± 5.26	44.20 ± 3.97	> 0.05

Data displayed as mean ± SD. $p > 0.05$ indicates no significant differences between trials.

Abbreviations: RT, rest trial; CT-1, cycling trial 1; CT-2, cycling trial 2.

and metabolic responses between trials.

Table 4. Mean Physiological responses during identical cycling trials

Experimental Trial			
Variable	**CT-1**	**CT-2**	**p-Value**
HR (bpm)	137 ± 16	135 ± 16	> 0.05
RPE	11.05 ± 1.92	10.84 ± 1.54	> 0.05
Affective Response	2.10 ± 1.13	2.50 ± 0.64	> 0.05
Average $\dot{V}O_2$ Uptake ($mL \cdot min^{-1}$)	2311 ± 337	2268 ± 333	> 0.05
Total Energy Expenditure (kcal)	1363 ± 207	1351 ± 198	> 0.05
Relative $\dot{V}O_2$ Uptake ($\%\dot{V}O_{2max}$)	67 ± 11	66 ± 11	> 0.05
Respiratory Exchange Ratio	0.89 ± 0.03	0.90 ± 0.02	> 0.05
Carbohydrate Oxidation (g/min)	1.86 ± 0.36	1.86 ± 0.38	> 0.05
Fat Oxidation (g/min)	0.41 ± 0.16	0.38 ± 0.12	> 0.05

Data displayed as mean ± SD. p > 0.05 indicates no significant differences between trials.

Abbreviations: CT-1, cycling trial 1; CT-2, cycling trial 2; HR, heart rate; RPE, rating of perceived exertion; $\dot{V}O_2$, rate of oxygen uptake.

Effects of CT-1 and CT-2 on Total White Blood Cell Concentrations

The average blood volume adjusted total white blood cell concentrations throughout CT-1 and CT-2 are displayed in Table 5. Total WBC ($p < 0.001$), neutrophil ($p < 0.001$) and monocyte ($p < 0.01$) concentrations significantly increased Post-Ex and remained elevated at Recovery. There was no significant increase in lymphocyte concentration Post-Ex ($p = 0.33$), and concentrations were similar between Pre-Ex and Recovery. There were no significant differences in any subset between trials or timepoint ($p > 0.05$), demonstrating consistent immunological responses between CT-1 and CT-2.

Effects of Cycling on T Cell Concentrations

To further examine the composition of the lymphocyte population, specifically T cell memory subsets, flow cytometry was subsequently employed. Blood volume adjusted concentrations of $CD4^+$ and $CD8^+$ T cells and their sub-populations (N, CM, EM, and TEMRA) are reported in Table 5 across REST, CT-1 and CT-2 to represent Pre-Ex, Post-Ex and Recovery respectively. There were increases in total $CD3^+$ ($p = 0.03$) and $CD8^+$ ($p = 0.008$), but not $CD4^+$ ($p = 0.07$) T cell concentrations. Within the $CD8^+$ population, these changes were driven by naïve ($p < 0.05$), EM $CD8^+$ ($p = 0.03$), and TEMRA $CD8^+$ ($p = 0.02$), but not CM T cells ($p = 0.33$). The concentrations of all $CD4^+$ ($p = 0.02$) and $CD8^+$ ($p < 0.04$) T cell subsets, except $CD4^+$ EM, significantly decreased at Recovery relative to Post-Ex, but these were not different to Pre-Ex ($p > 0.05$).

Table 5. Differences in Peripheral Blood Immune Cell Concentrations (cells/μL)

Experimental Trial				
Immune cell subset	**Pre-Ex**	**Post-Ex**	**Recovery**	**p-Value**
WBCs	5700 ± 1080[1,2]	9330 ± 1937[1]	9463 ± 1135[2]	< 0.001
Neutrophils	2913 ± 794[1,2]	6056 ± 1782[1]	6852 ± 1135[2]	< 0.001
Lymphocytes	1960 ± 457	2222 ± 582[3]	1803 ± 508[3]	< 0.01
Monocytes	490 ± 137[1,2]	691 ± 220[1]	577 ± 127[2]	< 0.01
T cells	701 ± 50[11]	1248 ± 507[1,3]	546 ± 462[3]	< 0.05
CD4+ T cells	435 ± 364	722 ± 304[3]	300 ± 279[3]	< 0.001
N	283 ± 280	430 ± 230[3]	177 ± 184[3]	< 0.001
CM	53 ± 35[1]	108 ± 47[1,3]	42 ± 32[3]	< 0.05
EM	92 ± 52	172 ± 135	76 ± 61	> 0.05
TEMRA	7 ± 5	12 ± 6[3]	5 ± 6[3]	< 0.05
CD8+ T cells	183 ± 140[1]	348 ± 165[1,3]	139 ± 107[3]	< 0.01
N	98 ± 75[1]	171 ± 95[1,3]	70 ± 48[3]	< 0.05
CM	7 ± 7	11 ± 7[3]	5 ± 4[3]	< 0.05
EM	63 ± 59[1]	116 ± 77[1,3]	49 ± 51[3]	< 0.05
TEMRA	15 ± 14[1]	50 ± 44[1,3]	15 ± 15[3]	< 0.05

Data displayed as mean ± SD. p > 0.05 indicates no significant differences between trials.
[1], significant difference between Pre-Ex and Post-Ex ($P < 0.05$)
[2], significant difference between Pre-Ex and Rec-Ex ($P < 0.05$)
[3], significant difference between Post-Ex and Rec-Ex ($P < 0.05$)

Abbreviations: Pre-Ex, pre-exercise; Post-Ex, post-exercise; Rec-Ex, Recovery-Exercise; WBC, white blood cell; N, Naïve; CM, central memory; EM, effector memory; TEMRA, terminally differentiated effector memory.

Mitochondrial Membrane Potential

ΔΨm for each T cell populations at Pre-Ex are reported in Supplementary Figure 2, expressed as a ratio of the raw MSO-MFI to the BAM-15 treated control. There were no differences between total lymphocytes, $CD3^+$, $CD4^+$ and $CD8^+$ T cells. Within $CD4^+$ T cells, EM exhibited greater ΔΨm than naïve cells ($p = 0.03$) and within $CD8^+$ T cells, ΔΨm was greater in CM than naïve cells ($p = 0.01$).

Relative changes in total $CD4^+$ and $CD8^+$ T cell ΔΨm (and associated daughter subpopulations) in response to prolonged cycling are shown in Figure 2A-D. There were no changes in ΔΨm between Pre-Ex and Post-Ex, except for an increase in naïve $CD8^+$ T cells ($p = 0.02$, Figure 2D). In Recovery relative to Pre-Ex, ΔΨm increased in total $CD3^+$ T cells ($p = 0.002$, Figure 2B), and this change was driven by increases within $CD8^+$ CM ($p = 0.03$), $CD4^+$ CM ($p = 0.02$) and EM ($p = 0.008$) subsets (Figures 2C-D). For absolute changes, there was an increase in ΔΨm of $CD4^+$ T cells between Pre-Ex and Recovery only ($p = 0.01$), driven by CM ($p = 0.03$) and EM ($p = 0.01$) subsets (Supplementary Figure 3B). There were no changes in mitochondrial mass in any cell type across any timepoint ($p > 0.05$).

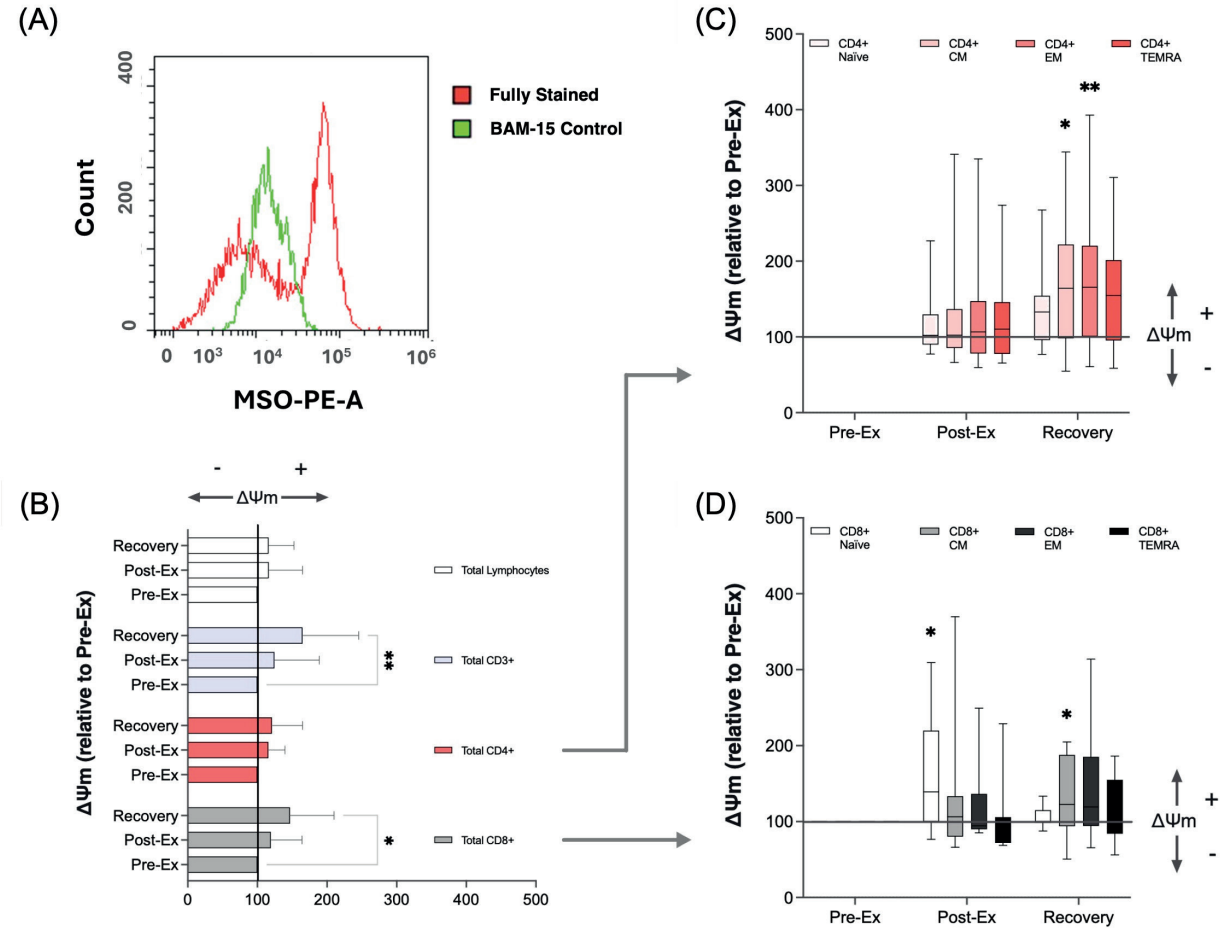

Figure 2. Relative changes in the mitochondrial membrane potential of T Cell subsets in response to prolonged cycling. ΔΨm was expressed as a ratio of the raw mean fluorescence intensity (MFI) of MitoSpy Orange (MSO) to the BAM-15 treated control. (A) Representative histograms depicting MSO-MFI of gated central memory CD4⁺ T cells treated with MSO (red) and BAM-15 + MSO (green). Changes in ΔΨm immediately and in recovery from cycling were expressed relative to Pre-Ex (Increase vs. Pre-Ex >100, Decrease vs. Pre-Ex <100) in total lymphocytes (light grey), CD3⁺ (purple), CD4⁺ (red) and CD8⁺ (dark grey) T cells (B). ΔΨm of naïve, CM, EM and TEMRA subsets (progressively darker colour representing antigen experience: TEMRA > EM > CM > naive) for (C) CD4+ (red) and (D) CD8⁺ T cells (grey) are also depicted. * represents significant differences between cell subsets: *p < 0.05, **p < 0.01.

Changes in the Metabolic Profile of PBMCs and Isolated Naïve T cells in Response to Prolonged Cycling

Purity of Enriched CD4⁺ and CD8⁺ Naïve T cells

The purity of naïve CD4⁺ and CD8⁺ T cells were confirmed by flow cytometry. Prior to enrichment, naïve (CD45RA⁺ CCR7⁻) CD4⁺ and CD8⁺ T cells composed 67.15% ± 16.08 and 52.12% ± 14.69 of the total T cell fraction respectively. After MACS enrichment, the mean frequencies of naïve CD4⁺ and CD8⁺ T cells were 98.85% ± 1.18 and 99.84% ± 0.14 respectively, indicating purity in line with manufacturer standards (> 95%). Subsequently, absolute (Figure 3) and relative (Figure 4) changes in the metabolic phenotypes of PBMCs and enriched naïve CD4⁺ and CD8⁺ T cells in response to prolonged cycling are presented. Immunometabolic outcomes for naïve CD4⁺ and CD8⁺ T cells are presented as a proportion of the PBMC fraction, based on compositional shifts in lymphocytes and monocytes elicited by cycling (Figure 3C–D). A full description of the latter is reported in Supplementary Materials.

Absolute Changes in Metabolic Parameters

Live-cell absolute measurements of OCR in response to modulators of mitochondrial respiration are presented in Figure 3B and used to calculate parameters of mitochondrial function (Figure 3E–I). There were no significant differences in basal, ATP-linked, maximal respiration, proton leak or spare respiratory capacity in naïve CD4⁺ and CD8⁺ T cells or PBMCs between Pre-Ex, Post-Ex and Recovery ($p > 0.05$). Real-time measurements of glycolytic flux (Figure 3J) and rates of ATP synthesis rates (Figure 3K–L) were not significantly changed in naïve CD4⁺ and CD8⁺ T cells, or PBMCs across timepoints. Across all absolute measurements, OCR, glycolytic PER and rates of ATP synthesis were significantly higher in PBMCs than all naïve T cells ($p < 0.0001$). To assist with data interpretation, 95% confidence intervals of the mean differences, effect sizes (Cohen's d) and F-statistics are presented in Supplementary Tables 1 and 2. There were consistent trends for an increase in all metabolic variables between Pre-Ex and Post-Ex for all cell subsets, demonstrating small (0.2 - 0.5) to moderate (0.5 – 0.8) effect sizes. Furthermore, there were consistent trends for a decrease in the same variables between Pre-Ex and Recovery, demonstrating moderate (0.5 – 0.8) to large effect sizes (> 0.8). However, the large confidence intervals indicate variable responses between participants.

Relative Changes in Metabolic Parameters

Measurements of OCR and PER in response to modulators of mitochondrial respiration were used to calculate the relative contributions of mitochondrial parameters within each cell fraction (Figure

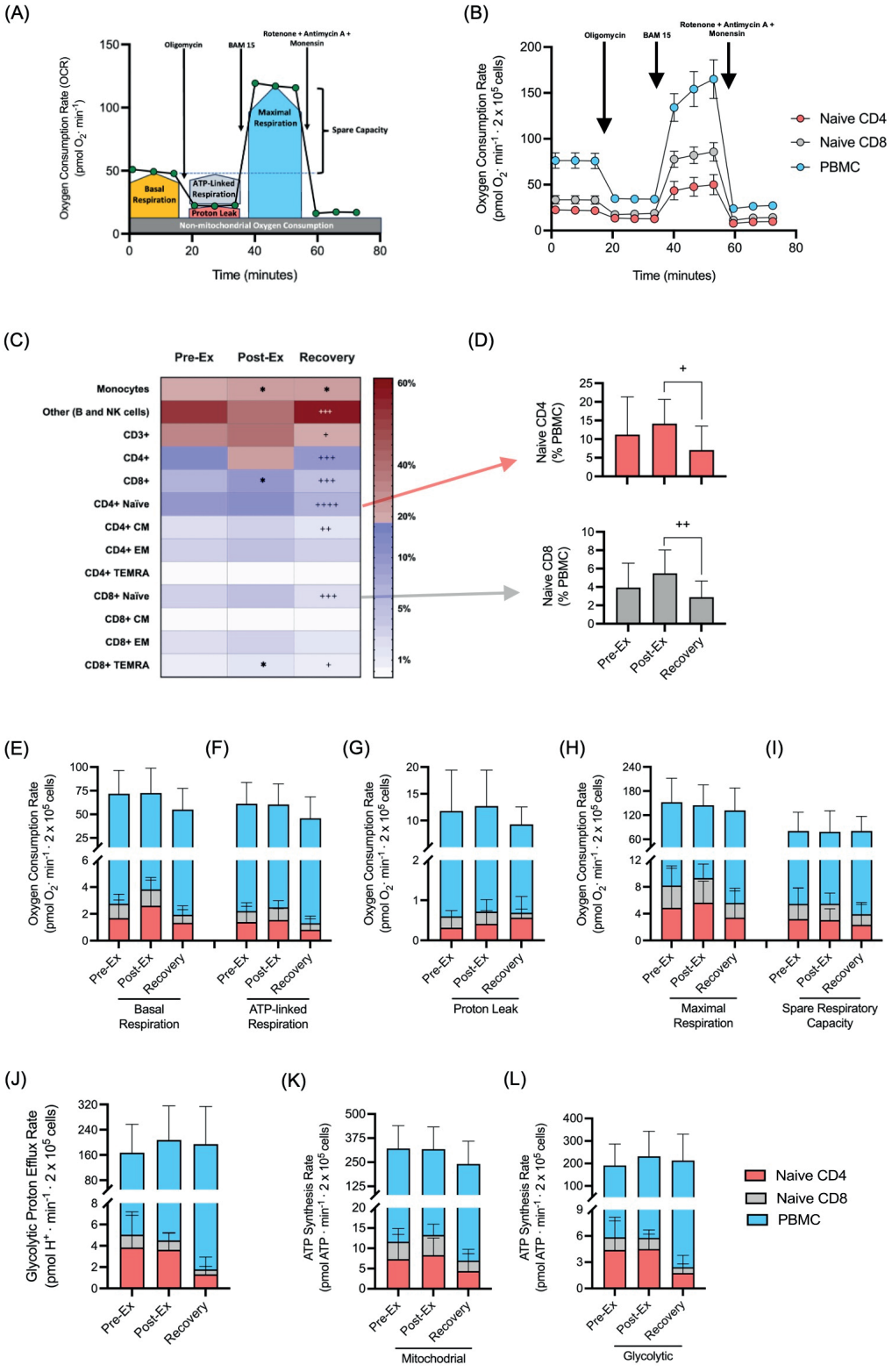

Figure 3. Mitochondrial profile of naïve CD4⁺ and CD8⁺ T cells within 200 x 10^3 seeded PBMCs/well. (A) Schematic representation of changes in oxygen consumption rate (OCR) monitored using a Seahorse XFe96 Analyzer when oligomycin, BAM 15 and rotenone + antimycin A + monensin were injected. Basal (yellow), ATP-linked (grey), maximal respiration (blue), proton leak (red), and spare respiratory capacity (blue) were calculated. (B) Representative live traces of OCR within naïve CD4⁺ T cells (red circles), CD8⁺ T cells (grey circles) and PBMCs (blue circles). OCR was measured continuously throughout the experimental period at baseline followed by the addition of the 3 indicated drugs. (C) A heat map presents the proportions of immune cell populations determined using flow cytometry within Pre-Ex, Post-Ex and Recovery PBMC samples. N.B. monocyte, B cell and NK cell frequencies were calculated from negative populations acquired during flow cytometry analysis and not directly using antibody conjugates. (D) Frequencies of naïve CD4⁺ and CD8⁺ T cells in seeded PBMCs from each timepoint for OCR measurement are graphically depicted. (E) Basal, (F) ATP-linked respiration, (G) Proton leak, (H) Maximal respiration, and (I) Spare respiratory capacity (J) Glycolytic PER, (K) Mitochondrial and (L) Glycolytic ATP production rates are presented for naïve CD4⁺ T cells (red stacked bars), CD8⁺ T cells (grey stacked bars) and PBMCs (total bar). N.B. Blue stacked bars represent values for 'PBMC – naïve CD4⁺ and CD8⁺ T cells'. Data presented as the mean ± SD of 10 participants x 3 timepoints. * indicates significant differences between Pre-Ex and Post-Ex or Recover, and + indicates significant differences between Post-Ex and Recovery: $p > 0.05$, *$p < 0.05$, **$p < 0.01$, +$p < 0.05$, ++$p < 0.01$, +++$p < 0.001$, ++++$p < 0.0001$. All immunometabolism outcomes were significantly greater in PBMCs vs. naïve T cells, but not indicated on every graph.

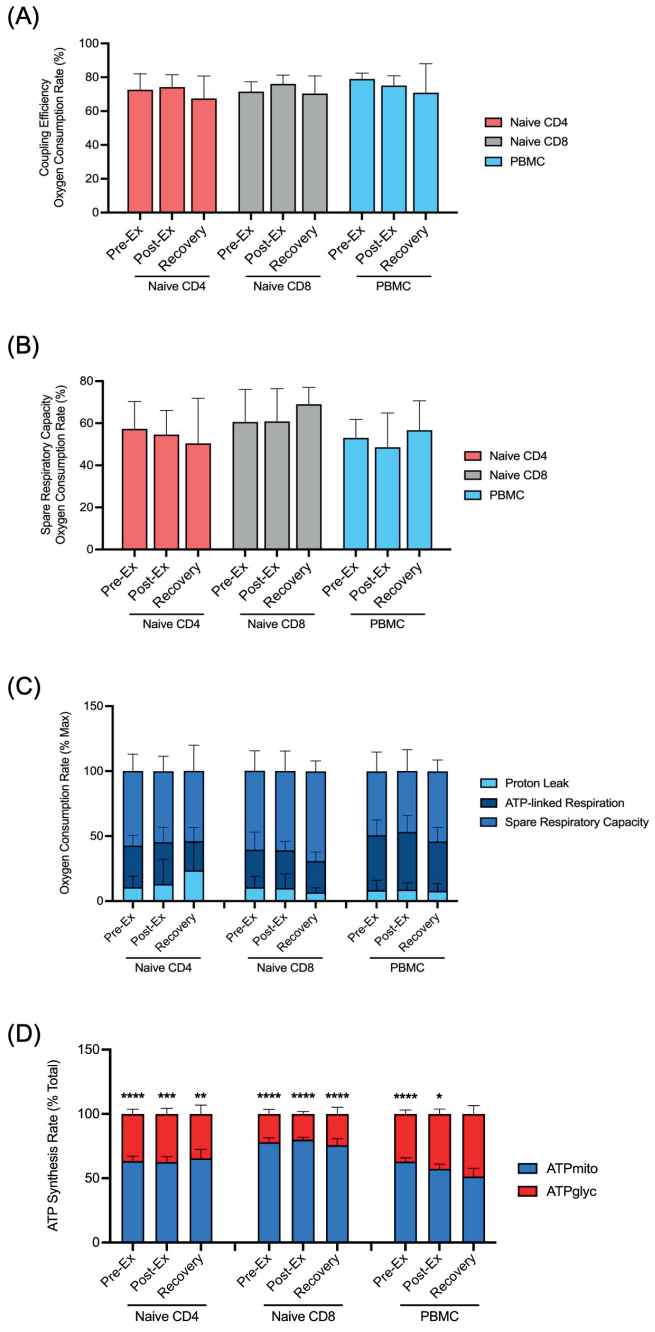

Figure 4. Relative changes in metabolic parameters (% maximal OCR) within isolated naïve CD4⁺ and CD8⁺ T cells vs. PBMCs in response to prolonged cycling. (A) Coupling Efficiency, (B) Spare Respiratory Capacity, (C) Differences in proton leak, ATP-linked respiration, and spare respiratory capacity and (D) ATP synthesis rate (% total). Data presented as the mean ± SD of 10 participants. * indicates significant differences between ATPmito and ATPglyc: $p > 0.05$, *$p < 0.05$, **$p < 0.01$, ***$p < 0.001$, ****$p < 0.0001$.

4). There were no significant differences in coupling efficiency (% basal OCR, Figure 4A) or spare respiratory capacity (% maximal OCR, Figure 4B) across timepoints ($p > 0.05$). Similarly, there were no changes observed in the proportional contributions of proton leak, ATP-leaked respiration and spare respiratory capacity (Figure 4C) in any cell type or between timepoints ($p > 0.05$). When comparing the relative contribution of glycolysis and mitochondrial respiration to ATP synthesis rate (Figure 4D), total ATP production was driven by mitochondrial respiration relative to glycolysis across all cell types ($p < 0.0001$), with the contribution greater in naïve T cells vs. PBMCs ($p = 0.0004$). This pattern was present across all timepoints, except PBMCs at recovery (% contribution, Pre-Ex: 62.8 ± 9.73, Post-Ex: 57.3 ± 11.88, and Recovery: 51.3 ± 20.27, $p = 0.29$). Although this indicates a shift in metabolic energy phenotype at this timepoint, there were no differences in mitochondrial or glycolytic driven ATP production between timepoints for naïve CD4⁺ ($p = 0.87$), naïve CD8⁺ ($p = 0.61$) T cells or PBMCs ($p = 0.29$). Tabular data, including 95% confidence intervals, effect sizes (Cohen's d) and F-statistics are presented in Supplementary Tables 2 and 3.

Effect of Prolonged Cycling on *Ex vivo* T cell Metabolic Profile upon Activation

Absolute Changes in Metabolic Parameters upon Stimulation

To determine real-time metabolic responses to T cell activation in collected blood samples, enriched naïve T cells and PBMCs were incubated with a CD3/CD28 activator. All samples were seeded at 2 x 105 cells per well, thus enriched naïve CD4⁺ and CD8⁺ T cell numbers were equal across Pre-Ex, Post-Ex and Recovery. However as expected, there were significant differences in the number of T cell subsets within the PBMC fraction across timepoints (Time x Cell subset Interaction: $F_{24,234} = 6.78$, $p < 0.0001$). These differences are graphically depicted in Figure 5A and a full description of the statistics given in Supplementary Tables 4 and 5.

In response to activation, there were significant increases in glycolytic PER (Figure 5F–H) and Supplementary Table 4) in all cell types at all timepoints and significant increases in glycolytic ATP synthesis rate, but not mitochondrial, across all timepoints for naïve CD4⁺ and Naïve CD8⁺ T cells but not PBMCs (Figure 5L-N and Supplementary Table 5). Across all timepoints, absolute PER was significantly greater in PBMCs (average pmol $H^+ \cdot min^{-1}$: 267.84 ± 129.41) vs. naïve CD4⁺ (average pmol $H^+ \cdot min^{-1}$: 70.01 ± 32.20) and CD8⁺ (average pmol $H^+ \cdot min^{-1}$: 41.49 ± 23.55) T cells ($F_{2,54} = 79.67$, $p < 0.0001$, Figure 5F-H). There were no exercise effects found for any variable from any cell type as values remained unaltered between timepoints ($p > 0.05$).

Prolonged Ex Vivo T-cell Stimulation

Two further indicators of naïve T cell activation upon *ex vivo* stimulation are increases in cell diameter (74), and secretion of IL-2, measured in the cell supernatant (10). In response to 12-hours of CD3/CD28 activation, the mean diameter of naïve CD4⁺ (µm, control: 6.37 ± 0.49 vs. activation: 7.50 ± 0.53, Main Effect of Condition: $p < 0.0001$) and CD8⁺ (µm, control: 6.05 ± 0.59 vs. activation: 7.95 ± 0.54, Main Effect of Condition: $p < 0.0001$) T cells significantly increased across all timepoints (Figure 6A–B), but there were no differences between timepoints ($p = 0.13$). The concentration of IL-2 (pg/mL) measured in the supernatant isolated from naïve CD4⁺ and naïve CD8⁺ T cells did not change after activation across all timepoints, ($F_{2,20} = 0.29$, $p = 0.75$ and $F_{2,29} = 0.20$, $p = 0.82$) (Figure 6C–D). There were no significant differences across timepoints ($p = 0.18$) and no correlation between changes in IL-2 concentration and PER in any cell type (Figure 6E–F).

Effect of Prolonged Cycling on Metabolic Substrates

To evaluate changes in circulating nutrient availability in response to prolonged moderate-intensity cycling, the concentrations of lactate, glucose, glutamine, and triglycerides were quantified (Figure 7A–C). There was no significant increase in lactate concentration

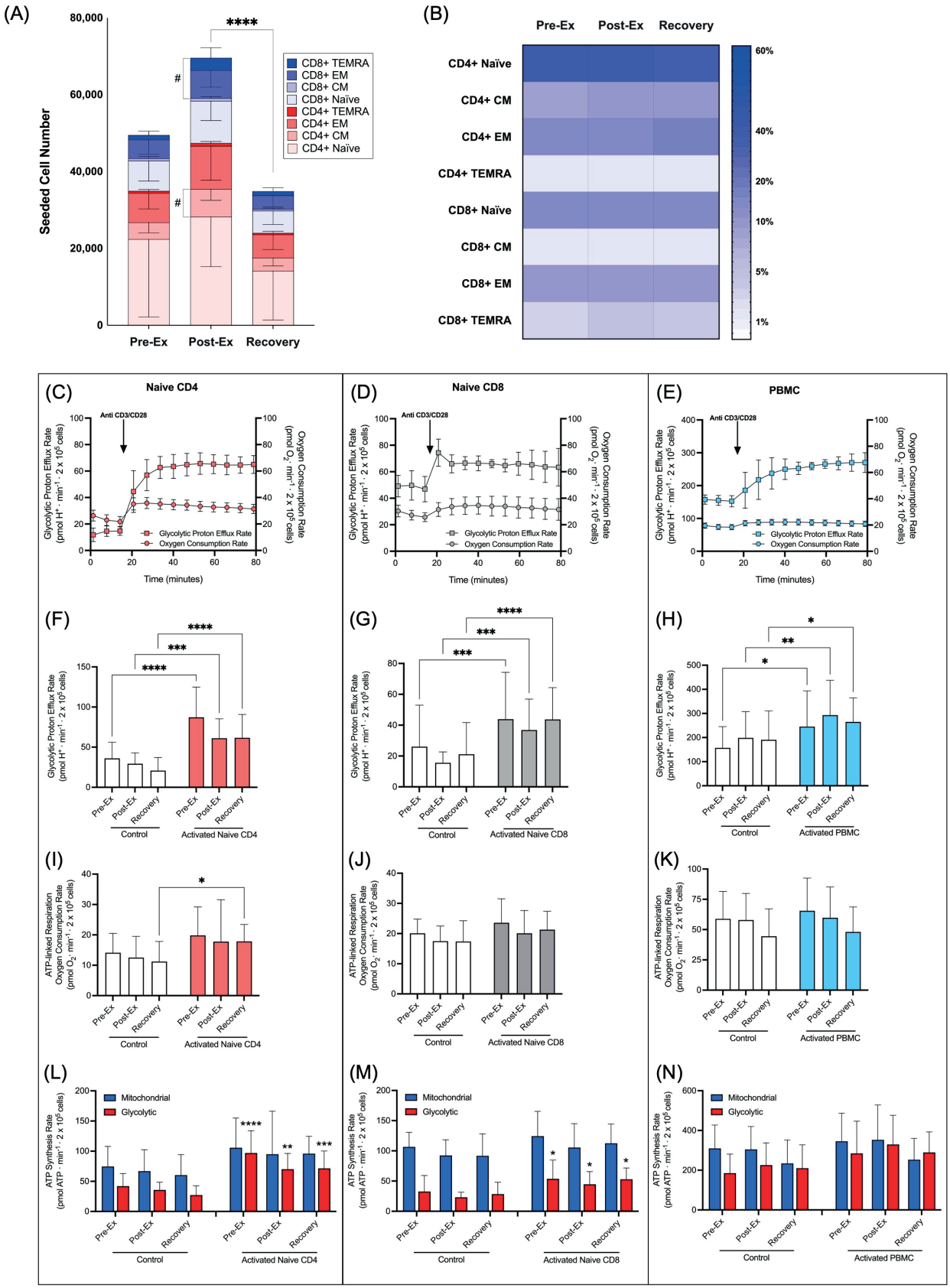

Figure 5. Real-time metabolic responses to CD3/CD28 activation within enriched naïve CD4⁺ and naïve CD8⁺ T cells, and PBMCs. (A) a stacked graph presents the numbers and (B) a heat map shows the frequency of T cell subsets within the seeded PBMC fraction for the activation assay. Representative traces of Glycolytic PER vs. Mitochondrial OCR upon activation of (C) Naïve CD4⁺, (D) Naïve CD8⁺ T cells, and (E) PBMCs were recorded with a Seahorse XFe96 Analyzer. CD3/CD28 activation beads were injected at 14 – 20 minutes, and PER was measured continuously throughout the experimental period after 3 measurements at baseline. (F–H) PER and (I–K) ATP-linked respiration of activated naïve CD4⁺ (red bars), naïve CD8⁺ (grey bars) T cells, and PBMCs (blue bars) vs. control (white bars) were then calculated. Differences in ATP synthesis rate between mitochondrial respiration (blue bars) and glycolysis (red bars) on (L) Naïve CD4⁺, (M) Naïve CD8⁺ T cells, and (N) PBMC. Data presented as the mean ± SD of 10 participants. # indicates significant differences between Pre-Ex and Post-Ex, and * indicates significant differences between timepoints or condition: $p > 0.05$, #$p < 0.05$, *$p < 0.05$, **$p < 0.01$, ***$p < 0.001$, ****$p < 0.0001$.

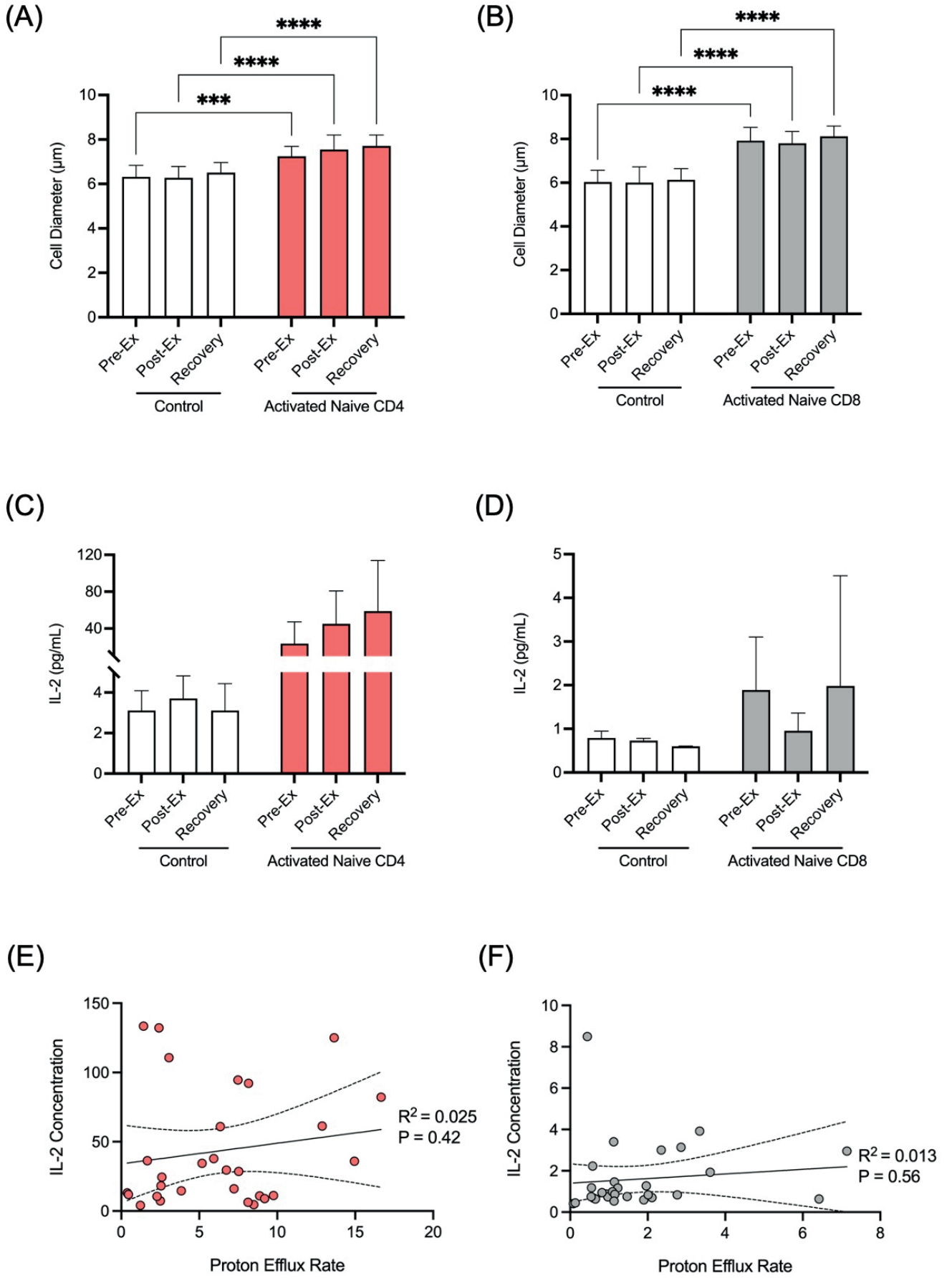

Figure 6. (A–B) Changes in cell diameter and (C–D) IL-2 secretion from naïve CD4⁺ T cells (red bars) and naïve CD8⁺ T cells (grey bars) after prolonged activation or control (white bars). A Pearson correlation between IL-2 concentration and PER are then indicated for (E) naïve CD4⁺ T cells (red circles) and (F) naïve CD8⁺ T cells (grey circles). Data presented as the mean ± SD of 10 participants. * indicates significant differences between control and activation: $p > 0.05$, ***$p < 0.001$, ****$p < 0.0001$.

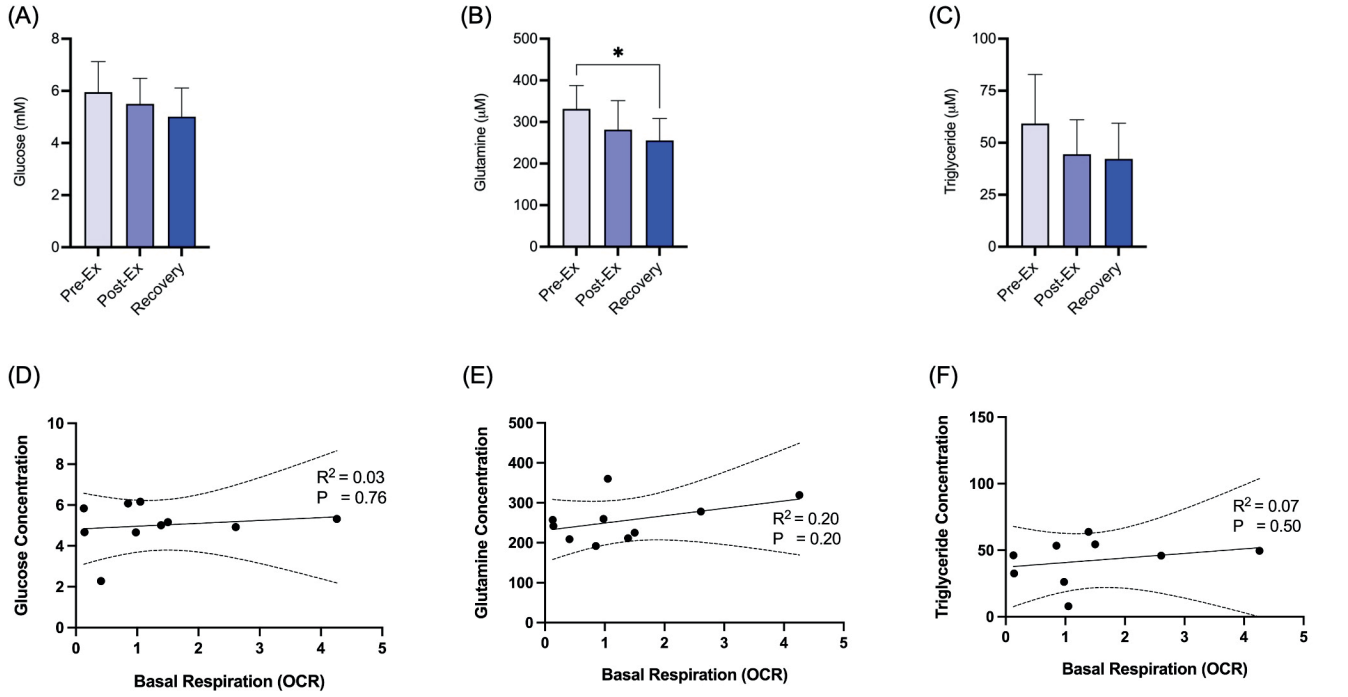

Figure 7. Concentrations of (A) glucose, (B) glutamine, and (C) triglycerides in response to prolonged cycling. (D–F) Representative correlations between each metabolite and basal respiration are provided. Data presented as the mean ± SD of 10 participants. * indicates significant differences between timepoints: $p > 0.05$, *$p < 0.05$.

from Rest (Pre-Ex: 1.83 ± 0.54 mmol/L) to the prescribed LT-1 exercise intensity domain (Average during exercise: 2.09 ± 0.39 mmol/L, $p = 0.25$). There were no differences in glucose ($F_{2,27} = 1.89$, $p = 0.17$) and triglyceride ($F_{2,25} = 2.17$, $p = 0.14$) concentrations across timepoints, but glutamine concentration (Figure 7B) significantly decreased at Recovery compared to Pre-Ex ($F_{2,27} = 4.17$, $p = 0.03$). There were no significant correlations between changes in plasma glucose, glutamine or triglyceride concentration and metabolic outcomes in all cell types across any timepoints.

DISCUSSION

This study investigated changes to the bioenergetic profile of T cells in response to prolonged moderate intensity cycling. The primary finding was that relative to rest, 2 hours of cycling at 95% LT1 elicited no marked changes to the immunometabolic profiles of naïve $CD4^+$ and $CD8^+$ T cells, or PBMCs immediately after and 2 hours into recovery. Using XF analysis, absolute and relative measures of mitochondrial respiration, glycolytic flux and ATP synthesis rate were similar across all timepoints. The contribution of mitochondrial respiration to ATP production was greater than glycolysis in naïve T cells across all timepoints and Pre-Ex and Post-Ex in PBMCs, but not Recovery. Using flow cytometry to further examine the mitochondrial activity of each T cell subset, the $\Delta\Psi m$ of $CD8^+$ and memory $CD4^+$ T cells was observed to be greater in Recovery vs. Rest. Functional T cell responses were preserved across all timepoints, with no changes in cellular bioenergetic responses after *ex vivo* CD3/CD28 activation in all cell fractions. Collectively, these data indicate that the metabolic phenotype and *ex vivo* responses to activation of the total PBMC fraction and isolated naïve T cells were largely unaltered within 2 hours of prolonged moderate intensity cycling.

The current study demonstrated an expected exercise-induced lymphocytosis (7, 23, 62, 79), with significantly greater concentrations of CM $CD4^+$ (+204%), and naïve (+174%), EM (+184%) and TEMRA $CD8^+$ T cells (+333%) in peripheral blood immediately after prolonged cycling at 95% LT1, relative to rest (Table 5). A pattern of preferential mobilisation of antigen experienced T cells was present for $CD8^+$ (TEMRA > EM > N), but not $CD4^+$ T cells. The mobilisation of antigen experienced T cells during bouts of exercise has been a reproducible finding in the field of exercise immunology (7, 29, 82) and relates to higher cell surface expression of beta-2 adrenergic receptor (19). The subsequent redeployment of these cells from the circulation is believed to govern immunosurveillance during recovery (37, 62, 67) and shifts in cellular metabolism have been proposed to facilitate this (3, 23, 34, 51, 72). Data from the present study indicate no marked changes in the bioenergetic profile of the total PBMC fraction immediately after prolonged moderate intensity cycling. This corroborates previous data indicating limited effect of moderate-to-vigorous intensity cycling (30 minutes at 65–70% $\dot{V}O_{2max}$) (75) or maximal swimming (72) on the mitochondrial respiratory function of PBMCs on a cell-by-cell basis. Interestingly, low-intensity cycling (~35% $\dot{V}O_{2peak}$) for 1 hour has been reported to increase fatty acid-dependent respiration in PBMCs (41), indicating metabolic sensitivity of PBMCs to acute exercise. When contrasting the current study design to Liepinsh et al, 2020, participants in our study were more aerobically trained ($\dot{V}O_{2max}$: 53.9 ± vs 33.3 ± 1.3), exercised at a substantially higher relative exercise intensity ($\dot{V}O_{2max}$: 66.1 ± 11.1 vs. 36.0 ± 1.8) and this resulted in less contribution of fat oxidation (Fat: Carbohydrate Oxidation Ratio: 0.22 ± 0.44 vs. 0.59 ± 0.43). Examination of fatty acid specific respiration (41) vs. real-time measurements of mitochondrial and glycolytic energy metabolism and carbohydrate specific respiration in other studies (72, 75) in part, explain

the observed inverse relationship between exercise intensity and PBMC respiration. However, lower intensity exercise would have perturbed peripheral blood immune composition to a lesser degree than in the present (Table 5, Figure 3C) and previous studies (72, 75). Examining cell-by-cell changes after more intense bouts of exercise, where leukocyte ingress/ egress is more marked and not uniform (23, 55, 62) makes examination of the cells of interest more challenging. Analysis 2 hours into recovery was a novel element of the present study design and our data indicate modulation of energy phenotype within PBMCs at this timepoint. The contribution of mitochondrial respiration to ATP production was significantly greater than glycolysis in PBMCs at rest and immediately after prolonged cycling; however, there was no difference in recovery (Figure 4D). This relative shift favouring greater glycolytic > mitochondrial contribution indicates an activated energy phenotype; however, there was no accompanying absolute changes in PER. Collectively, PBMC bioenergetics were largely unaltered within two hours of prolonged cycling. A conundrum persists when examining functional changes of the PBMC fraction after single bouts of exercise. This was exemplified by the notable compositional shifts in $CD4^+$ and $CD8^+$ N, CM, EM and TEMRA cells after cycling (Table 5, Figure 3C), underpinning the importance of providing single cell resolution on measures of cellular bioenergetics (27).

To overcome these challenges, the present study used immunomagnetic separation to enrich naïve T cells from the PBMC fraction and examine their metabolic phenotype and complemented by a flow cytometry assay that coupled immunophenotyping to measurements of ΔΨm. Rates of basal OCR (Figure 3E–I) and PER (Figure 5F–H) were substantially lower in naïve T cells vs. PBMCs and ΔΨm was lower in naïve vs. EM $CD4^+$ and CM $CD8^+$ T cells (Supplemental Figure 2). This confirms previous findings indicating greater mitochondrial and glycolytic respiration (17) and ΔΨm in antigen experienced vs. naive T cell subsets (73). These differences are independent of any effect of exercise, making interpretation of changes within the mixed PBMC fraction between timepoints challenging. However, similar to PBMCs, there were no statistically significant differences in the real-time metabolic profiles of enriched naïve $CD4^+$ and $CD8^+$ T cells either immediately or 2 hours after cessation of cycling, despite mean trends mirroring naïve T cell mobilisation patterns (supplementary Table 1). Specifically, absolute and relative OCR measures of basal, maximal and ATP-linked respiration, proton leak and spare respiratory capacity were unaltered (Figures 3E-I). Furthermore, rates of glycolysis nor the relative contributions of glycolysis and mitochondrial respiration to ATP synthesis rate significantly changed across timepoints (Figures 3J-L). In contrast, flow cytometry data revealed a relative increase in the ΔΨm of naïve $CD8^+$ T cells immediately after prolonged cycling (+43.0%, Figure 2D). Coupling MSO to immunophenotyping provides a reflection of total mitochondrial activity based on charge, rather than directly quantifying oxygen consumption rate during XF analysis (25). Similar dyes (5,5′,6,6′-tetrachloro-1,1′,3,3′-tetraethylbenzimidazolcarbocyanine iodide (JC-1)) have been used previously to examine changes in ΔΨm after bouts of exercise; however, measurements were only taken from the entire lymphocyte population based on forward vs. side scatter (78). Perhaps surprisingly, there were no significant changes in ΔΨm within CM, EM or TEMRA $CD4^+$ and $CD8^+$ T cells immediately after cycling (Figure 2C-D). The ΔΨm of these antigen experienced T cells was significantly greater than naive T cells at rest (Supplemental Figure 2) and therefore changes in the $CD8^+$ naïve T cell population may reflect an exercise-responsive increase in mitochondrial activity due to their quiescent state and greater metabolic flexibility compared to antigen experience T cells (69). In recovery, ΔΨm of CM $CD8^+$ (+30.7%) and CM (+66.7%) and EM $CD4^+$ T cells (+75.7%) were significantly elevated vs. Pre-Ex (Figure 2C-D). Mechanisms underpinning these cell specific changes are unclear. Circulating metabolites that support T cell function, namely glucose and triglyceride concentrations remained stable throughout the trial; however, there was a significant decrease in glutamine concentration in Recovery relative to Rest (Figure 7). This is well-documented after prolonged bouts of exercise (53, 59) and may relate to increased uptake by the liver to support acute phase protein production or notably, uptake from circulating active lymphocytes (22). It is well established that lymphocytes utilise glutamine during periods of stress (i.e., exercise) to provide energy for biosynthesis and to support cell proliferation (84). Although immune cell bioenergetics evaluated via EFA were largely resistant to the drop in plasma glutamine, we can speculatively suggest that the uptake of glutamine from the circulation may, in part, explain elevated ΔΨm of T cell memory subsets in recovery (15, 39).

To determine the impact of prolonged cycling on functional metabolic outcomes in naïve and PBMCs (naive and antigen experienced T cells - CM, EM and TEMRA), real-time metabolic responses to activation were examined *ex vivo* using a CD3/CD28 activator (Figure 5C–E). This approach enabled cellular bioenergetics to be profiled in real-time from activated T-cells within the PBMC fraction and enriched naïve T cells. In response to *ex vivo* activation, there was an increase in maximal glycolytic flux defined by PER, cell diameter, but not IL-2 production (Figures 5 and 6); however, there were no differences observed between timepoints, indicating that prolonged exercise didn't modulate T cell activation responses. Recent data indicates elevated activation-induced proliferation responses of $CD3^+$ T cells after high vs. moderate intensity exercise which may partly explain the lack of immunometabolic differences across timepoints (65). Further, a study by Withnall et al, 2024 indicated lower energetic demand and cytokine production from activated T cells (using PMA and ionomycin) isolated from physically active vs. inactive individuals (83). Our study cohort of aerobically trained participants may therefore demonstrate less sensitivity to metabolic reprogramming (via changes in PER) in T cells after prolonged cycling. This is challenging to interpret without a direct comparison with a sedentary control group.

FUTURE DIRECTIONS & LIMITATIONS

Collectively, these data indicate that bioenergetic profiles and metabolic responses to activation of naïve $CD4^+$ and $CD8^+$ T cells and the total PBMC fraction were largely unaltered in response to prolonged moderate intensity cycling. These analyses included measurements both immediately and 2 hours into recovery under controlled laboratory conditions, whereby nutrition (for 12 hours) and rest were controlled. It is noteworthy that recent studies employing single cell RNA sequencing have revealed pro-gly-

colytic shifts within mobilised EM T cells after bouts of exhaustive exercise (3), independent of shifts in cell composition. This study directly examined naïve T cells, due to their high proportion within the PBMC fraction and ease of isolation compared to antigen experienced T cells which are at a lower frequency (CM, EM, and TEMRA, Figure 3C). Although significant mobilisation of $CD8^+$ naïve T cells was reported in the present study, the preferential mobilisation of TEMRA > EM > CM > N (7, 29) highlights that comprehensive examination of antigen experienced T cell bioenergetics, and other cell types (e.g., NK cells, monocytes and B cells) after exercise bouts of different intensity is warranted. Our flow cytometry data provided some insight, revealing that mobilisation of antigen-experienced T cells was not accompanied by changes in $\Delta\Psi m$. Mitochondrial activity was higher in T memory cells in recovery (Figure 2) and this finding warrants further investigation.

Given the emerging literature in support of immune cell bioenergetic adaptions after exercise training (2, 32) it is important to highlight that our findings are restricted to aerobically trained males and females. Most participants in the current study would be classified as having 'Excellent' aerobic fitness based on their age category ($mL \cdot kg^{-1} \cdot min^{-1}$: male > 57.1, female > 46.5), as defined by American College of Sports Medicine (60). Our sample size was relatively small due to the logistical constraints of conducting extensive and detailed biological analysis. This prevented further stratification of data to examine sex-specific differences in acute bioenergetic responses to exercise. Recent studies have highlighted differences between males and females with regards to immunity and exercise (4, 14), although our initial data (N=5 vs. N=5) revealed no striking differences (data not shown). The changes in some bioenergetic variables exhibited moderate to large effect sizes and these should be explored in future studies using a larger sample size.

It is important to acknowledge limitations surrounding the examination of immunometabolic responses to bouts of exercise in humans. We adopted a study design that mitigated time spent processing peripheral blood samples to robustly examine immunometabolic responses in single T cell subsets. However, the time taken to collect, purify and analyse samples (≈ 3 hours) may have influenced cells in vivo metabolic state, despite the rigorous control measures employed. All cells were washed into standardised glucose rich media (i.e. RPMI), but future studies could consider autologous serum as a media to better preserve the bioenergetic state of isolated cells *ex vivo* (18).

Many previous studies examining immunometabolic responses to bouts of exercise have mostly defined 'intensity' based on a proportion of $\dot{V}O_{2max}$ (40), which doesn't account for inter-individual variation in metabolic thresholds that occur at different stages of $\dot{V}O_{2max}$ (40). The current study therefore used 95% LT1 to prescribe a metabolically controlled bout of cycling near aerobic threshold. At this intensity, exercise can be sustained for prolonged durations with minimal fatigue and metabolite (e.g. lactate and adrenaline) accumulation (9, 30). An ongoing narrative in exercise immunology literature purports that prolonged arduous exercise (≥ 2 hours) may impair aspects of immune function (8, 48–50, 68). For the current study population of aerobically trained young males and females, 2 hours of cycling at a moderate intensity (66.1 ± 11.1 % $\dot{V}O_{2max}$) was subjectively perceived as 'fairly light' (RPE: 11.1 ± 1.9) and 'fairly good' (affective response: 2.5 ± 0.6) for physical exertion and enjoyment respectively, despite significant energy expenditure (1357 ± 203 kcal). Although not 'arduous', these data indicate that despite robust T cell mobilisation in response to prolonged cycling, bioenergetic responses were unaltered, therefore providing no evidence to indicate impairment of immune function within 2 hours of recovery, most notably in naïve T cells. To further address this question, future studies should utilise these single cell methods to examine immunometabolic outcomes after more intense bouts or periods of exercise training.

CONCLUSION

These data indicate no marked perturbations in naïve $CD4^+$ and $CD8^+$ T cell or PBMC bioenergetics either immediately or 2 hours after cycling. There was an increase in the mitochondrial membrane potential of memory $CD4^+$ and $CD8^+$ T cells 2 hours following cycling and this finding warrants further investigation.

ETHICS STATEMENT

The study was given favourable ethical opinion by the Science, Technology, Engineering and Mathematics ethical committee at the University of Birmingham (ERN_19-1574PA3).

AUTHOR CONTRIBUTIONS

AJW conceptualised the study and provided project direction. JPB, AJW and FP designed Seahorse experiments. AJW, JS, NG and SKD designed $\Delta\Psi m$ flow cytometry assays. FP and JS carried out all data acquisition. GAW and TP provided insight on study design. Data analyses and presentation were carried out by FP, JB and AJW. AJW interpreted the data and drafted the manuscript, with support from FP. All authors undertook the revision and final approval of the manuscript. Artificial Intelligence (AI) was not used in any aspect of the study, writing or otherwise.

FUNDING

This project was supported by a scholarship grant from the Indonesian Endowment Fund for Education awarded to FP and supervised by AJW. Funding was also provided by a grant from the Society for Endocrinology awarded to AJW.

CONFLICT OF INTEREST

None of the authors declare a conflict of interest.

SUPPLEMENTARY MATERIALS

Link to be added.

REFERENCES

1. Alley JR, Valentine RJ, Kohut ML. Mitochondrial Mass of Naïve T Cells Is Associated with Aerobic Fitness and Energy Expenditure of Active and Inactive Adults. Medicine and Science in Sports and Exercise 54: 1288–1299, 2022. doi: 10.1249/MSS.0000000000002914.
2. Andonian BJ, Koss A, Koves TR, Hauser ER, Hubal MJ, Pober DM, Lord JM, MacIver NJ, St Clair EW, Muoio DM, Kraus WE, Bartlett DB, Huffman KM. Rheumatoid arthritis T cell and muscle oxidative metabolism associate with exercise-induced changes in cardiorespiratory fitness. Scientific Reports 12, 2022. doi: 10.1038/s41598-022-11458-4.
3. Batatinha H, Diak DM, Niemiro GM, Baker FL, Smith KA, Zúñiga TM, Mylabathula PL, Seckeler MD, Lau B, LaVoy EC, Gustafson MP, Katsanis E, Simpson RJ. Human lymphocytes mobilized with exercise have an anti-tumor transcriptomic profile and exert enhanced graft-versus-leukemia effects in xenogeneic mice. Frontiers in Immunology 14: 1–14, 2023. doi: 10.3389/fimmu.2023.1067369.
4. Bauza DER, Silveyra P. Sex Differences in Exercise-Induced Effects on Respiratory Infection and Immune Function. .
5. Bisset S. Effect of Muscular Activity prior to Venepuncture on the Respiration of Leucocytes in vitro. 1958.
6. Burke LM, Hawley JA, Wong SHS, Jeukendrup AE. Carbohydrates for training and competition. Journal of Sports Sciences 29, 2011. doi: 10.1080/02640414.2011.585473.
7. Campbell JP, Riddell NE, Burns VE, Turner M, van Zanten JJCSV, Drayson MT, Bosch JA. Acute exercise mobilises $CD8^+$ T lymphocytes exhibiting an effector-memory phenotype. Brain, Behavior, and Immunity 23: 767–775, 2009. doi: 10.1016/j.bbi.2009.02.011.
8. Campbell JP, Turner JE. Debunking the Myth of Exercise-Induced Immune Suppression: Redefining the Impact of Exercise on Immunological Health Across the Lifespan. Frontiers in Immunology 9: 1–21, 2018. doi: 10.3389/fimmu.2018.00648.
9. Cannon DT, White AC, Andriano MF, Kolkhorst FW, Rossiter HB. Skeletal muscle fatigue precedes the slow component of oxygen uptake kinetics during exercise in humans. Journal of Physiology 589: 727–739, 2011. doi: 10.1113/jphysiol.2010.197723.
10. Cantrell DA, Smith KA. The Interleukin-2 T-Cell System: A New Cell Growth Model [Online]. www.sciencemag.org.
11. Carney CE, Buysse DJ, Ancoli-Israel S, Edinger JD, Krystal AD, Lichstein KL, Morin CM. The consensus sleep diary: Standardizing prospective sleep self-monitoring. Sleep 35: 287–302, 2012. doi: 10.5665/sleep.1642.
12. Chapman NM, Shrestha S, Chi H. Metabolism in immune cell differentiation and function. 2017.
13. Cohen J. Statistical Power Analysis for the Behavioral Sciences, 2nd Edition. 1988.
14. Cortes CJ, De Miguel Z. Precision Exercise Medicine: Sex Specific Differences in Immune and CNS Responses to Physical Activity. Brain Plasticity 8: 65–77, 2022. doi: 10.3233/bpl-220139.
15. Cruzat V, Rogero MM, Keane KN, Curi R, Newsholme P. Glutamine: Metabolism and immune function, supplementation and clinical translation. Nutrients 10, 2018. doi: 10.3390/nu10111564.
16. Deyhle MR, Gier AM, Evans KC, Eggett DL, Nelson WB, Parcell AC, Hyldahl RD. Skeletal muscle inflammation following repeated bouts of lengthening contractions in humans. Frontiers in Physiology 6, 2016. doi: 10.3389/fphys.2015.00424.
17. Dimeloe S, Mehling M, Frick C, Loeliger J, Bantug GR, Sauder U, Fischer M, Belle R, Develioglu L, Tay S, Langenkamp A, Hess C. The Immune-Metabolic Basis of Effector Memory $CD4^+$ T Cell Function under Hypoxic Conditions. The Journal of Immunology 196: 106–114, 2016. doi: 10.4049/jimmunol.1501766.
18. Dorneles GP, da Silva IM, Santos MA, Elsner VR, Fonseca SG, Peres A, Romão PRT. Immunoregulation induced by autologous serum collected after acute exercise in obese men: a randomized cross-over trial. Scientific Reports 10: 1–16, 2020. doi: 10.1038/s41598-020-78750-z.
19. Fan X, Wang Y. β2 Adrenergic receptor on T lymphocytes and its clinical implications. Progress in Natural Science 19: 17–23, 2009. doi: 10.1016/j.pnsc.2008.10.001.
20. Field CJ, Gougeon R, Marliss EB. Circulating mononuclear cell numbers and function during intense exercise and recovery. Journal of Applied Physiology 71: 1089–1097, 1991. doi: 10.1152/jappl.1991.71.3.1089.
21. Foster J. The General Practice Physical Activity Questionnaire (GPPAQ) A screening tool to assess adult physical activity levels , within primary care Updated May 2009. Nhs : 1–21, 2009.
22. Gleeson M. The Journal of Nutrition 7th Amino Acid Assessment Workshop Dosing and Efficacy of Glutamine Supplementation in Human Exercise and Sport Training 1,2. 2008.
23. Graff RM, Kunz HE, Agha NH, Baker FL, Laughlin M, Bigley AB, Markofski MM, LaVoy EC, Katsanis E, Bond RA, Bollard CM, Simpson RJ. β2-Adrenergic receptor signaling mediates the preferential mobilization of differentiated subsets of $CD8^+$ T-cells, NK-cells and non-classical monocytes in response to acute exercise in humans. Brain, Behavior, and Immunity 74: 143–153, 2018. doi: 10.1016/j.bbi.2018.08.017.
24. Gubser PM, Bantug GR, Razik L, Fischer M, Dimeloe S, Hoenger G, Durovic B, Jauch A, Hess C. Rapid effector function of memory $CD8^+$ T cells requires an immediate-early glycolytic switch. Nature Immunology 14: 1064–1072, 2013. doi: 10.1038/ni.2687.
25. Gudgeon N, Munford H, Bishop EL, Hill J, Fulton-Ward T, Bending D, Roberts J, Tennant DA, Dimeloe S. Succinate uptake by T cells suppresses their effector function via inhibition of mitochondrial glucose oxidation. Cell Reports 40, 2022. doi: 10.1016/j.celrep.2022.111193.
26. Hardy CJ, Rejeski WJ. Not What, but How One Feels: The Measurement of Affect during Exercise. Journal of Sport and Exercise Psychology 11: 304–317, 2016. doi: 10.1123/jsep.11.3.304.
27. Hodgman CF, Hunt RM, Crane JC, Elzayat MT, LaVoy E. A Scoping Review on the Effects of Physical Exercise and Fitness on Peripheral Leukocyte Energy Metabolism in Humans. 29: 54–87, 2023. doi: 10.1136/bmj.n71.
28. Howley ET, Bassett Jr DR, Welch HG. Criteria for maximal oxygen uptake: review and commentary. Medicine & Science in Sports & Exercise, 27(9), 27: 1292-1301.-1292-1301., 1995.
29. Hunt RM, Elzayat MT, Markofski MM, Laughlin M, LaVoy EC. Characterization of transitional memory $CD4^+$ and $CD8^+$ T-cell mobilization during and after an acute bout of exercise. Frontiers in Sports and Active Living 5, 2023. doi: 10.3389/fspor.2023.1120454.
30. Iannetta D, Inglis EC, Mattu AT, Fontana FY, Pogliaghi S, Keir DA, Murias JM. A Critical Evaluation of Current Methods for Exercise Prescription in Women and Men. Medicine and Science in Sports and Exercise 52: 466–473, 2020. doi: 10.1249/MSS.0000000000002147.
31. Jamnick NA, Pettitt RW, Granata C, Pyne DB, Bishop DJ. An Examination and Critique of Current Methods to Determine Exercise Intensity. Sports Medicine 50: 1729–1756, 2020. doi: 10.1007/s40279-020-01322-8.

32. Janssen JJE, Lagerwaard B, Porbahaie M, Nieuwenhuizen AG, Savelkoul HFJ, Van Neerven RJJ, Keijer J, De Boer VCJ. Extracellular flux analyses reveal differences in mitochondrial PBMC metabolism between high-fit and low-fit females. American Journal of Physiology - Endocrinology and Metabolism 322, 2022. doi: 10.1152/AJPENDO.00365.2021.
33. Jeukendrup AE, Wallis GA. Measurement of Substrate Oxidation During Exercise by Means of Gas Exchange Measurements [Online]. doi: 10.1055/s-2004-830512.
34. Jones N, Piasecka J, Bryant AH, Jones RH, Skibinski DOF, Francis NJ, Thornton CA. Bioenergetic analysis of human peripheral blood mononuclear cells. Clinical and Experimental Immunology 182: 69–80, 2015. doi: 10.1111/cei.12662.
35. Jones N, Cronin JG, Dolton G, Panetti S, Schauenburg AJ, Galloway SAE, Sewell AK, Cole DK, Thornton CA, Francis NJ. Metabolic adaptation of human $CD4^+$ and $CD8^+$ T-cells to T-cell receptor-mediated stimulation. Frontiers in Immunology 8, 2017. doi: 10.3389/fimmu.2017.01516.
36. Keir DA, Iannetta D, Mattioni Maturana F, Kowalchuk JM, Murias JM. Identification of Non-Invasive Exercise Thresholds: Methods, Strategies, and an Online App. Sports Medicine 52: 237–255, 2022. doi: 10.1007/s40279-021-01581-z.
37. Krüger K, Lechtermann A, Fobker M, Völker K, Mooren FC. Exercise-induced redistribution of T lymphocytes is regulated by adrenergic mechanisms. Brain, Behavior, and Immunity 22: 324–338, 2008. doi: 10.1016/j.bbi.2007.08.008.
38. La Rocca C, Carbone F, De Rosa V, Colamatteo A, Galgani M, Perna F, Lanzillo R, Brescia Morra V, Orefice G, Cerillo I, Florio C, Maniscalco GT, Salvetti M, Centonze D, Uccelli A, Longobardi S, Visconti A, Matarese G. Immunometabolic profiling of T cells from patients with relapsing-remitting multiple sclerosis reveals an impairment in glycolysis and mitochondrial respiration. Metabolism: Clinical and Experimental 77: 39–46, 2017. doi: 10.1016/j.metabol.2017.08.011.
39. Lai AG, Forde D, Chang WH, Yuan F, Zhuang X, Rubio CO, Song CX, McKeating JA. Glucose and glutamine availability regulate HepG2 transcriptional responses to low oxygen . Wellcome Open Research 3, 2018. doi: 10.12688/wellcomeopenres.14839.1.
40. Lei TH, Wang IL, Chen YM, Liu XH, Fujii N, Koga S, Perry B, Mundel T, Wang F, Cao Y, Dobashi K, Kondo N, Li HY, Goulding RP. Critical power is a key threshold determining the magnitude of post-exercise hypotension in non-hypertensive young males. Experimental Physiology 108: 1409–1421, 2023. doi: 10.1113/EP091429.
41. Liepinsh E, Makarova E, Plakane L, Konrade I, Liepins K, Videja M, Sevostjanovs E, Grinberga S, Makrecka-Kuka M, Dambrova M. Low-intensity exercise stimulates bioenergetics and increases fat oxidation in mitochondria of blood mononuclear cells from sedentary adults. Physiological Reports 8, 2020. doi: 10.14814/phy2.14489.
42. Lin ML, Hsu CC, Fu TC, Lin YT, Huang YC, Wang JS. Exercise Training Improves Mitochondrial Bioenergetics of Natural Killer Cells. Medicine and Science in Sports and Exercise 54: 751–760, 2022. doi: 10.1249/MSS.0000000000002842.
43. Lovakov A, Agadullina ER. Empirically derived guidelines for effect size interpretation in social psychology. European Journal of Social Psychology 51: 485–504, 2021. doi: 10.1002/ejsp.2752.
44. Matomäki P, Kainulainen H, Kyröläinen H. Corrected whole blood biomarkers – the equation of Dill and Costill revisited. Physiological Reports 6: 1–3, 2018. doi: 10.14814/phy2.13749.
45. Mercier-Letondal P, Marton C, Godet Y, Galaine J. Validation of a method evaluating T cell metabolic potential in compliance with ICH Q2 (R1). Journal of Translational Medicine 19, 2021. doi: 10.1186/s12967-020-02672-7.
46. Morgado JP, Matias CN, Reis JF, Curto D, Alves FB, Monteiro CP. The Cellular Composition of the Innate and Adaptive Immune System Is Changed in Blood in Response to Long-Term Swimming Training. Frontiers in Physiology 11: 1–10, 2020. doi: 10.3389/fphys.2020.00471.
47. Nicoli F, Papagno L, Frere JJ, Cabral-Piccin MP, Clave E, Gostick E, Toubert A, Price DA, Caputo A, Appay V. Naïve $CD8^+$ t-cells engage a versatile metabolic program upon activation in humans and differ energetically from memory $CD8^+$ T-cells. Frontiers in Immunology 9: 1–12, 2018. doi: 10.3389/fimmu.2018.02736.
48. Nieman DC, Henson DA, Dumke CL, Lind RH, Shooter LR, Gross SJ. Relationship between salivary IgA secretion and upper respiratory tract infection following a 160-km race. The Journal of sports medicine and physical fitness 46: 158–162, 2006.
49. Nieman DC, Johanssen LM, Lee JW, Arabatzis K. Infectious episodes in runners before and after the Los Angeles Marathon. Journal of Sports Medicine and Physical Fitness 30: 316–328, 1990.
50. Nieman DC. Is infection risk linked to exercise workload? Medicine and Science in Sports and Exercise 32, 2000. doi: 10.1097/00005768-200007001-00005.
51. Nieman DC, Lila MA, Gillitt ND. Immunometabolism: A Multi-Omics Approach to Interpreting the Influence of Exercise and Diet on the Immune System. Annual Review of Food Science and Technology 10: 341–363, 2019. doi: 10.1146/annurev-food-032818-121316.
52. Oertelt-Prigione S. Immunology and the menstrual cycle. Autoimmunity Reviews 11, 2012. doi: 10.1016/j.autrev.2011.11.023.
53. Parry-Billings M, Budgett R, Koutedakis Y, Blomstrand E, Brooks S, Williams C, Calder PC, Pilling S, Baigrie R, Newsholme EA. Plasma amino acid concentrations in the overtraining syndrome: possible effects on the immune system. Medicine and science in sports and exercise 12: 1353–1358, 1992.
54. Perry SW, Norman JP, Barbieri J, Brown EB, Gelbard HA. Mitochondrial membrane potential probes and the proton gradient: A practical usage guide. BioTechniques 50: 98–115, 2011. doi: 10.2144/000113610.
55. Pradana F, Nijjar T, Cox PA, Morgan PT, Podlogar T, Lucas SJE, Drayson MT, Kinsella FAM, Wadley AJ. Brief cycling intervals incrementally increase the number of hematopoietic stem and progenitor cells in human peripheral blood. Frontiers in Physiology 15, 2024. doi: 10.3389/fphys.2024.1327269.
56. Rangel Rivera GO, Knochelmann HM, Dwyer CJ, Smith AS, Wyatt MM, Rivera-Reyes AM, Thaxton JE, Paulos CM. Fundamentals of T Cell Metabolism and Strategies to Enhance Cancer Immunotherapy. Frontiers in Immunology 12, 2021. doi: 10.3389/fimmu.2021.645242.
57. Rathmell JC, Heiden MGV, Harris MH, Frauwirth KA, Thompson CB. In the absence of extrinsic signals, nutrient utilization by lymphocytes is insufficient to maintain either cell size or viability. Molecular Cell 6: 683–692, 2000. doi: 10.1016/S1097-2765(00)00066-6.
58. Reina-Campos M, Scharping NE, Goldrath AW. $CD8^+$ T cell metabolism in infection and cancer. Nature Reviews Immunology 21: 718–738, 2021. doi: 10.1038/s41577-021-00537-8.
59. Rennie MJ, Edwards RH, Krywawych S, Davies CT, Halliday D, Waterlow JC, Millward DJ. Effect of exercise on protein turnover in man. 1981.

60. Riebe D, Ep-c A, Ehrman JK, Liguori G, Magal M. ACSM's guidelines for exercise testing and prescription. 10th ed. Wolters Kluwer Health, 2018.
61. Robert B, Brown EB. Psychophysical bases of perceived exertion. Medicine & Science in Sports & Exercise 14: 377–381, 1982.
62. Rooney BV, Bigley AB, LaVoy EC, Laughlin M, Pedlar C, Simpson RJ. Lymphocytes and monocytes egress peripheral blood within minutes after cessation of steady state exercise: A detailed temporal analysis of leukocyte extravasation. Physiology and Behavior 194: 260–267, 2018. doi: 10.1016/j.physbeh.2018.06.008.
63. Rothschild-Rodriguez D, Causer AJ, Brown FF, Collier-Bain HD, Moore S, Murray J, Turner JE, Campbell JP. The effects of exercise on complement system proteins in humans: a systematic scoping review. 2022.
64. Scharping NE, Menk AV, Moreci RS, Whetstone RD, Dadey RE, Watkins SC, Ferris RL, Delgoffe GM. The Tumor Microenvironment Represses T Cell Mitochondrial Biogenesis to Drive Intratumoral T Cell Metabolic Insufficiency and Dysfunction. Immunity 45: 374–388, 2016. doi: 10.1016/j.immuni.2016.07.009.
65. Siedlik JA, Deckert JA, Dunbar AJ, Bhatta A, Gigliotti NM, Chan MA, Benedict SH, Bubak M, Vardiman JP, Gallagher PM. Acute high-intensity exercise enhances T cell proliferation compared to moderate-intensity exercise. Applied Physiology, Nutrition, and Metabolism 50: 1–12, 2025. doi: 10.1139/apnm-2024-0420.
66. Simpson RJ, Bigley AB, Agha N, Hanley PJ, Bollard CM. Mobilizing immune cells with exercise for cancer immunotherapy. Exercise and Sport Sciences Reviews 45: 163–172, 2017. doi: 10.1249/JES.0000000000000114.
67. Simpson RJ, Boßlau TK, Weyh C, Niemiro GM, Batatinha H, Smith KA, Krüger K. Exercise and adrenergic regulation of immunity. Brain, Behavior, and Immunity 97: 303–318, 2021. doi: 10.1016/j.bbi.2021.07.010.
68. Simpson RJ Campbell, JP, Gleeson, M, Krüger,K, Nieman, DC,. Pyne, DB, Turner, JE, and Walsh, NP. Can exercise affect immune function to increase susceptibility to infection? Journal of applied sport psychology 26: 8–22, 2020.
69. Slack M, Wang T, Wang R. T cell metabolic reprogramming and plasticity. Molecular Immunology 68: 507–512, 2015. doi: 10.1016/j.molimm.2015.07.036.
70. Sottnik JL, Lori JC, Rose BJ, Thamm DH. Glycolysis inhibition by 2-deoxy-d-glucose reverts the metastatic phenotype in vitro and in vivo. Clinical and Experimental Metastasis 28: 865–875, 2011. doi: 10.1007/s10585-011-9417-5.
71. Spielberger CD, Gonzalez-Reigosa F, Martinez-Urrutia A, Natalicio LFS, Natalicio DS. The State-Trait Anxiety Inventory. Revista Interamericana de Psicología/Interamerican Journal of Psychology 5, 2017. doi: 10.30849/rip/ijp.v5i3.
72. Stampley JE, Cho E, Wang H, Theall B, Johannsen NM, Spielmann G, Irving BA. Impact of maximal exercise on immune cell mobilization and bioenergetics. Physiological Reports 11: 1–10, 2023. doi: 10.14814/phy2.15753.
73. Sukumar M, Liu J, Mehta GU, Patel SJ, Roychoudhuri R, Crompton JG, Klebanoff CA, Ji Y, Li P, Yu Z, Whitehill GD, Clever D, Eil RL, Palmer DC, Mitra S, Rao M, Keyvanfar K, Schrump DS, Wang E, Marincola FM, Gattinoni L, Leonard WJ, Muranski P, Finkel T, Restifo NP. Mitochondrial Membrane Potential Identifies Cells with Enhanced Stemness for Cellular Therapy. Cell Metabolism 23: 63–76, 2016. doi: 10.1016/j.cmet.2015.11.002.
74. Tasnim H, Fricke GM, Byrum JR, Sotiris JO, Cannon JL, Moses ME. Quantitative measurement of naïve T cell association with dendritic cells, FRCs, and blood vessels in lymph nodes. Frontiers in Immunology 9, 2018. doi: 10.3389/fimmu.2018.01571.
75. Theall B, Stampley J, Cho E, Granger J, Johannsen NM, Irving BA, Spielmann G. Impact of acute exercise on peripheral blood mononuclear cells nutrient sensing and mitochondrial oxidative capacity in healthy young adults. Physiological Reports 9, 2021. doi: 10.14814/phy2.15147.
76. Thomas DT, Erdman KA, Burke LM. Nutrition and Athletic Performance. Medicine and Science in Sports and Exercise 48: 543–568, 2016. doi: 10.1249/MSS.0000000000000852.
77. Toth MJ, Goran MI, Ades PA, Howard DB, Poehlman ET. Examination of data normalization procedures for expressing peak VO, data [Online]. www.physiology.org/journal/jappl.
78. Tuan TC, Hsu TG, Fong MC, Hsu CF, Tsai KKC, Lee CY, Kong CW. Deleterious effects of short-term, high-intensity exercise on immune function: Evidence from leucocyte mitochondrial alterations and apoptosis. British Journal of Sports Medicine 42: 11–15, 2008. doi: 10.1136/bjsm.2006.029314.
79. Turner JE, Wadley AJ, Aldred S, Fisher JP, Bosch JA, Campbell JP. Intensive Exercise Does Not Preferentially Mobilize Skin-Homing T Cells and NK Cells. Medicine and Science in Sports and Exercise 48: 1285–1293, 2016. doi: 10.1249/MSS.0000000000000914.
80. van der Windt GJW, Everts B, Chang CH, Curtis JD, Freitas TC, Amiel E, Pearce EJ, Pearce EL. Mitochondrial Respiratory Capacity Is a Critical Regulator of CD8 + T Cell Memory Development. Immunity 36: 68–78, 2012. doi: 10.1016/j.immuni.2011.12.007.
81. Voss K, Hong HS, Bader JE, Sugiura A, Lyssiotis CA, Rathmell JC. A guide to interrogating immunometabolism. Nature Reviews Immunology 21: 637–652, 2021. doi: 10.1038/s41577-021-00529-8.
82. Wadley AJ, Cullen T, Vautrinot J, Keane G, Bishop NC, Coles SJ. High intensity interval exercise increases the frequency of peripheral PD-1+ $CD8^+$ central memory T-cells and soluble PD-L1 in humans. Brain, Behavior, & Immunity - Health 3: 100049–100049, 2020. doi: 10.1016/j.bbih.2020.100049.
83. Withnall E, Hazeldine J, Llibre A, Duggal NA, Lord JM, Sardeli AV. Physical activity modifies the metabolic profile of $CD4^+$ and $CD8^+$ T cell subtypes at rest and upon activation in older adults. .
84. Yaqoob P, And D, Calder PC. Glutamine Requirement of Proliferating T Lymphocytes. OElsevier Science Inc, 1997.
85. World Medical Association Declaration of Helsinki: ethical principles for medical research involving human subjects. The Journal of the American College of Dentists 81: 14–18, 2014.